OXIDE SURFACES

edited by
James A. Wingrave
University of Delaware
Newark, Delaware

MARCEL DEKKER

MARCEL DEKKER, INC. NEW YORK · BASEL

2

Adsorbed and Grafted Polymers at Equilibrium

ROLAND R. NETZ Max-Planck-Institute for Colloids and Interfaces, Potsdam, Germany

DAVID ANDELMAN Tel Aviv University, Tel Aviv, Israel

I. INTRODUCTION

In this chapter, we review the basic mechanisms underlying adsorption of long-chain molecules on solid surfaces such as oxides. We concentrate on the physical aspects of adsorption and summarize the main theories which have been proposed. This chapter should be viewed as a general introduction to the problem of polymer adsorption at thermodynamical equilibrium. For a selection of previous review articles see Refs 1–4, while more detailed treatments are presented in two books on this subject [5, 6]. We do not attempt to explain any specific polymer/oxide system and do not emphasize experimental results and techniques. Rather, we detail how concepts taken from statistical thermodynamics and interfacial science can explain general and *universal* features of polymer adsorption. The present chapter deals with equilibrium properties whereas Chapter 3 by Cohen Stuart and de Keizer is about kinetics.

A. Types of Polymers

The polymers considered here are taken as linear and long chains, such as schematically depicted in Fig. 1a. We do not address the more complicated case of branched polymers at interfaces, although a considerable amount of work has been done on such systems [7]. In Fig. 1b we schematically present an example of a branched polymer. Moreover, we examine mainly homopolymers where the polymers are composed of the same repeated unit (monomer). We discuss separately, in Section VIII, extensions to adsorption of block copolymers and to polymers that are terminally grafted to the surface on one side ("polymer brushes"). In most of this review we shall assume that the chains are neutral. The charged case, i.e., where each or a certain fraction of monomers carries an electric charge, as depicted in Fig. 1c, is still not very well understood and depends on additional parameters such as the surface charge density, the polymer charge, and the ionic strength of the solution. We address shortly adsorption of polyelectrolytes in Section V. Furthermore, the chains are considered to be flexible. The statistical thermodynamics of flexible chains is rather well developed and the theoretical concepts can be applied with a considerable degree of confidence. Their large number of conformations play a crucial role in the

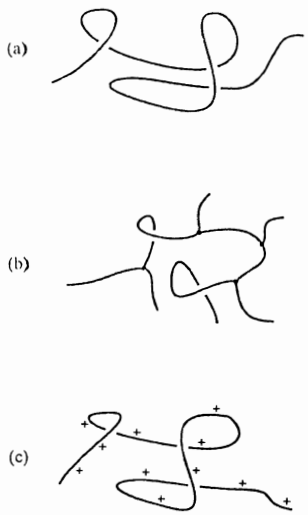

FIG. 1 Schematic view of different polymers. (a) Linear homopolymers, which are the main subject of this chapter; (b) branched polymers; (c) charged polymers or polyelectrolytes, with a certain fraction of charged groups.

adsorption, causing a rather *diffusive* layer extending away from the surface into the solution. This is in contrast to rigid chains, which usually form dense adsorption layers on surfaces.

B. Solvent Conditions

Polymers in solution can experience three types of solvent conditions. The solvent is called "good" when the monomer–solvent interaction is more favorable than the monomer–monomer one. Single polymer chains in good solvents have "swollen" spatial configurations, reflecting the effective repulsion between monomers. In the opposite case of "bad" (sometimes called "poor") solvent conditions, the effective interaction between monomers is attractive, leading to collapse of the chains and to their precipitation from the solution (phase separation between the polymer and the solvent). In the third and intermediate solvent condition, called "theta" solvent, the monomer–solvent and monomer–monomer interactions are equal in strength. The chains are still soluble, but their spatial configurations and solution properties differ from the good-solvent case.

The theoretical concepts and methods leading to these three classes make up a large and central part of polymer physics and are summarized in textbooks [7–12]. In general, the solvent quality depends mainly on the specific chemistry determining the interaction between the solvent molecules and monomers. It also can be changed by varying the temperature.

C. Adsorption and Depletion

Polymers can adsorb spontaneously from solution on to surfaces if the interaction between the polymer and the surface is more favorable than that of the solvent with the surface. For example, a polymer like poly(ethylene oxide) (PEO) is soluble in water but will adsorb on various hydrophobic surfaces and on the water/air interface. This is the case of equilibrium adsorption where the concentration of the polymer monomers increases close to the surface with respect to their concentration in the bulk solution. We discuss this phenomenon at length both on the level of a single polymer chain (valid only for extremely dilute polymer solutions), see Section II, and for polymers adsorbing from (semidilute) solutions, see Section III. In Fig. 2a we schematically show the volume fraction profile $\phi(z)$ of monomers as a function of the distance z from the adsorbing substrate. In the bulk, i.e., far away from the substrate surface, the volume fraction of the monomers is ϕ_b, whereas, at the surface, the corresponding value is $\phi_s > \phi_b$. The theoretical models address questions in relation to the polymer conformations at the interface, the local concentration of polymer in the vicinity of the surface, and the total amount of adsorbing polymer chains. In turn, the knowledge of the polymer interfacial behavior is used to calculate

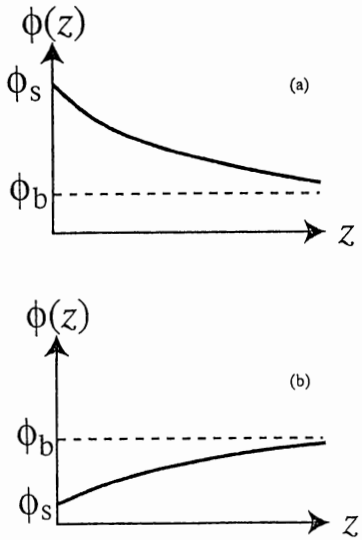

FIG. 2 Schematic profile of the monomer volume fraction $\phi(z)$ as a function of the distance z from a flat substrate as appropriate: (a) for the case of adsorption, where the substrate attracts monomers, leading to an increase in the polymer concentration close to the wall; and (b) for the case of depletion, where the substrate repels the monomers, leading to a decrease of the polymer concentration close to the wall. The symbol ϕ_b denotes the bulk volume fraction, i.e., the monomer volume fraction infinitely far away from the wall, and ϕ_s denotes the surface volume fraction right at the substrate surface.

thermodynamical properties like the surface tension in the presence of polymer adsorption.

The opposite case of *depletion* occurs when the monomer–surface interaction is less favorable than the solvent–surface interaction. This is, e.g., the case for polystyrene in toluene, which is depleted from a mica substrate. The depletion layer is defined as the layer adjacent to the surface from which the polymers are depleted. Their concentration in the vicinity of the surface is lower than the bulk value, as shown schematically in Fig. 2b.

D. Surface–Polymer Interactions

Equilibrium adsorption of polymers is only one of the methods used to create a change in the polymer concentration close to a surface. For an adsorbed polymer, it is interesting to look at the detailed conformation of a single polymer chain at the substrate. One distinguishes sections of the polymer which are bound to the surface, so-called trains, sections which form loops, and the end sections of the polymer chain, which can form dangling tails. This is schematically depicted in Fig. 3a. Two other methods to produce polymer layers at surfaces are commonly used for polymers which do not spontaneously adsorb on a given surface.

1. In the first method, the polymer is chemically attached (grafted) to the surface by one of the chain ends, as shown in Fig. 3b. In good solvent conditions the polymer chains look like "mushrooms" on the surface when the distance between grafting points is larger than the typical size of the chains. In some cases, it is possible to induce a much higher density of the grafting, resulting in a polymer "brush" extending in the perpendicular direction from the surface, as is discussed in detail in Section VIII.

2. A variant on the grafting method is to use a diblock copolymer made out of two distinct blocks, as shown in Fig. 3c. The first block is insoluble and is attracted to the substrate, and thus acts as an "anchor" fixing the chain to the surface; it is drawn as a thick line in Fig. 3c. It should be long enough to cause irreversible fixation on the surface. The other block is a soluble one (the "buoy"), forming the brush layer. For example, fixation on hydrophobic surfaces from a water solution can be made using a polystyrene–poly(ethylene oxide) (PS–PEO) diblock copolymer. The PS block is insoluble in water and is attracted towards the substrate, whereas the PEO forms the

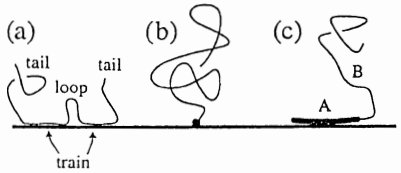

FIG. 3 The different adsorption mechanisms discussed in this chapter. (a) Adsorption of a homopolymer, where each monomer has the same interaction with the substrate; the "tail," "train," and "loop" sections of the adsorbing chain are shown. (b) Grafting of an end-functionalized polymer via a chemical or a physical bond. (c) Adsorption of a diblock copolymer where one of the two blocks is attached to the substrate surface, while the other is not.

brush layer. The process of diblock copolymer fixation has a complex dynamics during the formation stage, but is very useful in applications [10].

E. Surface Characteristics

Up to now we have outlined the polymer properties. What about the surface itself? Clearly, any adsorption process will be sensitive to the type of surface and its internal structure. As a starting point we assume that the solid surface is atomically smooth, flat, and homogeneous, as shown in Fig. 4a. This ideal solid surface is impenetrable to the chains and imposes on them a surface interaction. The surface potential can be short ranged, affecting only the monomers which are in direct contact with the substrate or in close vicinity of the surface. In other cases, the surface can have a longer range effect, like van der Waals, or electrostatic interactions, if it is charged.

Interesting extensions beyond ideal surface conditions are expected in several situations: (1) rough or corrugated surfaces, such as depicted in Fig. 4b; (2) surfaces that are curved, e.g., adsorption on spherical colloidal particles, see Fig. 4c; (3) substrates that are chemically inhomogeneous, i.e., which show some lateral organization, as shown schematically in Fig. 4d; (4) surfaces that have internal degrees of freedom like surfactant monolayers; and (5) polymers adsorbing on "soft" and

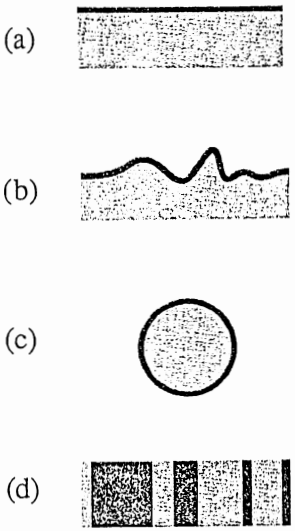

FIG. 4 Different possibilities of substrates. (a) The prototype, a flat, homogeneous substrate. (b) A corrugated, rough substrate; note that experimentally, every substrate exhibits some degree of roughness on some length scale. (c) A spherical adsorption substrate, such as a colloidal particle; if the colloidal radius is much larger than the polymer size, curvature effects (which means the deviation from the planar geometry) can be neglected. (d) A flat but chemically heterogeneous substrate.

"flexible" interfaces between two immiscible fluids or at the liquid/air surface. We briefly mention those situations in Sections V–VII.

F. Polymer Physics

Before turning to the problem of polymer adsorption let us briefly mention some basic principles of polymer theory. For a more detailed exposure the reader should consult the books by Flory, de Gennes, or Des Cloizeaux and Jannink [8, 11, 12]. The main parameters needed to describe a flexible polymer chain are the polymerization index N, which counts the number of repeat units or monomers, and the Kuhn length a, which corresponds to the spatial size of one monomer or the distance between two neighboring monomers. The monomer size ranges from 1.5 Å, as for example for polyethylene, to a few nanometers for biopolymers [8]. In contrast to other molecules or particles, a polymer chain contains not only translational and rotational degrees of freedom, but also a vast number of conformational degrees of freedom. For typical polymers, different conformations are produced by torsional rotations of the polymer backbone bonds, as shown schematically in Fig. 5a for a polymer consisting of three bonds of length a each. A satisfactory description of flexible chain conformations is achieved with the (bare) statistical weight for a polymer consisting of $N + 1$ monomers:

$$\mathscr{P}_N = \exp\left\{-\frac{3}{2a^2}\sum_{i=1}^{N}(\mathbf{r}_{i+1} - \mathbf{r}_i)^2\right\} \tag{1}$$

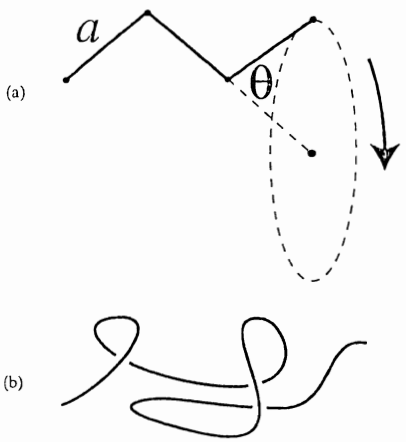

FIG. 5 (a) A polymer chain can be described as a chain of bonds of length a, with fixed torsional angles θ, reflecting the chemical bond structure, but otherwise freely rotating joints. (b) The simplified model, appropriate for theoretical calculations, consists of a structureless line, governed by some bending rigidity or line tension; this model chain is used when the relevant length scales are much larger than the monomer size, a.

which assures that each bond vector, given by $\mathbf{r}_{i+1} - \mathbf{r}_i$ with $i = 1, \ldots, N$, treated for convenience as a fluctuating Gaussian variable, has a mean length given by the Kuhn length, i.e.,

$$\langle(\mathbf{r}_i - \mathbf{r}_{i+1})^2\rangle = a^2$$

In most theoretical approaches, it is useful to take the simplification one step further and represent the polymer as a continuous line, as shown in Fig. 5b, with the statistical weight for each conformation given by Eq. (1) in the continuum limit. The Kuhn length a in this limit loses its geometric interpretation as the monomer size, and simply becomes an elastic parameter which is tuned such as to ensure the proper behavior of the large-scale properties of this continuous line, as is detailed below. Additional effects, a local bending rigidity, preferred bending angles (as relevant for *trans-gauche* isomery encountered for saturated carbon backbones), and hindered rotations can be taken into account by defining an effective polymerization index and an effective Kuhn length. In that sense, we always talk about effective parameters N and a, without saying so explicitly. Clearly, the total polymer length in the completely extended configuration is $L = aN$. However, the average spatial extent of a polymer chain in solution is typically much smaller. An important quantity characterizing the size of a polymer coil is the average end-to-end radius R_e. For the simple Gaussian polymer model defined above, we obtain:

$$R_e^2 = \langle(\mathbf{r}_{N+1} - \mathbf{r}_1)^2\rangle = a^2N \tag{2}$$

In a more general way, one describes the scaling behavior of the end-to-end radius for large values of N as $R_e \sim aN^{\nu}$. For an ideal polymer chain, i.e., for a polymer whose individual monomers do not interact with each other, the above result implies $\nu = 1/2$. This result holds only for polymers where the attraction between monomers (as compared with the monomer–solvent interaction) cancels the steric repulsion due to the impenetrability of monomers. This situation can be achieved in special solvent conditions called "theta" solvent as was mentioned above. In a theta solvent, the polymer chain is not as swollen as in good solvents but is not collapsed on itself either, as it is under bad solvent conditions.

For good solvents, the steric repulsion dominates and the polymer coil takes a much more open structure, characterized by an exponent $\nu \simeq 3/5$ [8]. The general picture that emerges is that the typical spatial size of a polymer coil is much smaller than the extended length $L = aN$, but larger than the size of the ideal chain $aN^{1/2}$. The reason for this peculiar behavior is entropy combined with the favorable interaction between monomers and solvent molecules in good solvents. The number of polymer configurations having a small end-to-end radius is large, and these configurations are entropically favored over configurations characterized by a large end-to-end radius, for which the number of possible polymer conformations is drastically reduced. It is this conformational freedom of polymer coils which leads to salient differences between polymer adsorption and that of simple liquids.

Finally, in bad solvent conditions, the polymer and the solvent are not compatible. A single polymer chain collapses on itself in order to minimize the monomer–solvent interaction. It is clear that in this case, the polymer size, like any space filling object, scales as $N \sim R_e^3$, yielding $\nu = 1/3$.

II. SINGLE-CHAIN ADSORPTION

Let us consider now the interaction of a single polymer chain with a solid substrate. The main effects particular to the adsorption of polymers (as opposed to the adsorption of simple molecules) are due to the reduction of conformational states of the polymer at the substrate, which is due to the impenetrability of the substrate for monomers [13–18]. The second factor determining the adsorption behavior is the substrate–monomer interaction. Typically, for the case of an adsorbing substrate, the interaction potential $V(z)$ between the substrate and a single monomer has a form similar to the one shown in Fig. 6, where z measures the distance of the monomer from the substrate surface:

$$V(z) \simeq \begin{cases} \infty & \text{for } z < 0 \\ -U & \text{for } 0 < z < B \\ -bz^{-\tau} & \text{for } z > B \end{cases} \tag{3}$$

The separation of $V(z)$ into three parts is done for convenience. It consists of a hard wall at $z = 0$, which embodies the impenetrability of the substrate, i.e., $V(z) = \infty$ for $z < 0$. For positive z we assume the potential to be given by an attractive well of depth U and width B. At large distances, $z > B$, the potential can be modeled by a long-ranged attractive tail decaying as $V(z) \sim -bz^{-\tau}$.

For the important case of (unscreened and nonretarded) van der Waals interactions between the substrate and the polymer monomers, the potential shows a decay governed by the exponent $\tau = 3$ and can be attractive or repulsive, depending on the solvent, the chemical nature of the monomers, and the substrate material. The decay power $\tau = 3$ follows from the van der Waals pair interaction, which decays as the inverse sixth power with distance, by integrating over the three spatial dimensions of the substrate, which is supposed to be a semi-infinite half-space [19].

The strength of the potential well is measured by $U/(k_B T)$, i.e., by comparing the potential depth U with the thermal energy $k_B T$. For strongly attractive potentials, i.e., for large U or, equivalently, for low temperatures, the polymer is strongly adsorbed and the thickness of the adsorbed layer, D, approximately equals the potential range B. The resulting polymer structure is shown in Fig. 7a, where the width of the potential well, B, is denoted by a broken line.

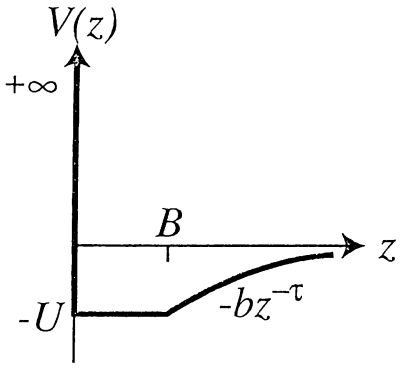

FIG. 6 A typical surface potential felt by a monomer as a function of the distance z from an adsorbing wall. First, the wall is impenetrable; then, the attraction is of strength U and range B. For separations larger than B, typically a long-ranged tail exists and is modeled by $-bz^{-\tau}$.

For weakly attractive potentials, or for high temperatures, we anticipate a weakly adsorbed polymer layer, with a diffuse layer thickness D much larger than the potential range B. This structure is depicted in Fig. 7b. For both cases shown in Fig. 7, the polymer conformations are unperturbed on a spatial scale of the order of D; on larger length scales, the polymer is broken up into decorrelated *polymer blobs* [11, 12], which are denoted by dotted circles in Fig. 7. The idea of introducing polymer blobs is related to the fact that very long and flexible chains have different spatial arrangements at small and large length scales. Within each blob the short-range interaction is irrelevant, and the polymer structure inside the blob is similar to the structure of an unperturbed polymer far from the surface. Since all monomers are connected, the blobs themselves are linearly connected and their spatial arrangement represents the behavior on large length scales. In the adsorbed state, the formation of each blob leads to an entropy loss of the order of one $k_B T$ (with a numerical prefactor of order unity, which is neglected in this scaling argument), so the total entropy loss of a chain of N monomers is $\mathcal{F}_{\text{rep}} \sim k_B T(N/g)$, where g denotes the number of monomers inside each blob.

Using the scaling relation $D \simeq ag^{\nu}$ for the blob size dependence on the number of monomers g, the entropy penalty for the confinement of a polymer chain to a width D above the surface can be written as [20]

$$\frac{\mathcal{F}_{\text{rep}}}{k_B T} \simeq N\left(\frac{a}{D}\right)^{1/\nu} \tag{4}$$

The adsorption behavor of a polymer chain results from a competition between the attractive $V(z)$, which tries to bind the monomers to the substrate, and the entropic

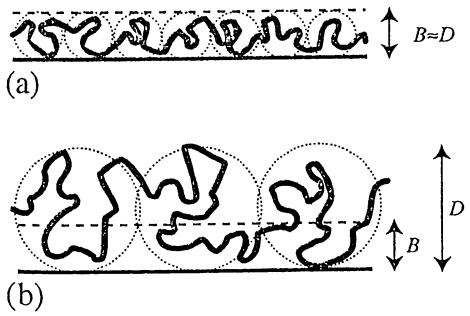

FIG. 7 Schematic drawing of single-chain adsorption: (a) in the limit of strong coupling, the polymer decorrelates into a whole number of blobs (shown as dotted circles) and the chain is confined to a layer thickness D, of the same order of magnitude as the potential range B; (b) in the case of weak coupling, the width of the polymer layer D is much larger than the interaction range B and the polymer forms large blobs, within which the polymer is not perturbed by the surface.

repulsion $\mathcal{F}_{\rm rep}$, which tries to maximize entropy and, therefore, favors a delocalized state where a large fraction of the monomers are located farther away from the surface.

It is of interest to compare the adsorption of long-chain polymers with the adsorption of small molecular solutes. Small molecules adsorb on to a surface only if there is a bulk reservoir with nonzero concentration in equilibrium with the surface. An infinite polymer chain $N \to \infty$ behaves differently as it remains adsorbed also in the limit of zero bulk concentration. This corresponds to a true thermodynamic phase transition in the limit $N \to \infty$ [21]. For a finite polymer length, however, the equilibrium behavior is, in some sense, similar to the adsorption of small molecules, and a nonzero bulk polymer concentration is needed for the adsorption of polymer chains on the substrate. For fairly long polymers, the desorption of a single polymer is almost a "true" phase transition, and corrections due to finite (but long) polymer length are often below experimental resolution.

A. Mean-Field Regime

Fluctuations of the local monomer concentration are of importance to the description of polymers at surfaces owing to the many possible chain conformations. These fluctuations are treated theoretically using field-theoretical or transfer-matrix techniques. In a field-theoretical formalism, the problem of accounting for different polymer conformations is converted into a functional integral over different monomer–concentration profiles [12]. Within transfer-matrix techniques, the Markov-chain property of ideal polymers is exploited to re-express the conformational polymer fluctuations as a product of matrices [22].

However, there are cases where fluctuations in the local monomer concentration become unimportant. The adsorption behavior of a single polymer chain is then obtained using simple *mean-field theory* arguments. Mean-field theory is a very useful approximation applicable in many branches of physics, including polymer physics. In a nutshell, each monomer is placed in a "field", generated by the averaged interaction with all the other monomers.

The mean-field theory can be justified for two cases: (1) a *strongly adsorbed polymer chain*, i.e., a polymer chain which is entirely confined inside the potential well; and (2) the case of *long-ranged attractive surface potentials*. To proceed, we assume that the adsorbed polymer layer is confined with an average thickness D, as depicted in Fig. 7a or 7b. Within mean-field theory, the polymer chain experiences an average of the surface potential, $\langle V(z)\rangle$, which is replaced by the potential evaluated at the average distance from the surface, $\langle z\rangle \simeq D/2$. Therefore, $\langle V(z)\rangle \simeq V(D/2)$. Further stringent conditions when such a mean-field theory is valid are detailed below. The full free energy of one chain, $\mathcal{F}$, of polymerization index N, can be expressed as the sum of the repulsive entropic term, Eq. (4), and the average potential:

$$\frac{\mathcal{F}}{k_{\rm B}T} \simeq N\left(\frac{a}{D}\right)^{1/\nu} + N\frac{V(D/2)}{k_{\rm B}T} \tag{5}$$

Let us consider first the case of a strongly adsorbed polymer, confined to a potential well of depth $-U$. In this case the potential energy per monomer becomes

$V(D/2) \simeq -U$. Comparing the repulsive entropic term with the potential term, we find the two terms to be of equal strength for a well depth $U^* \simeq k_{\rm B}T(a/D)^{1/\nu}$. Hence, the strongly adsorbed state, which is depicted in Fig. 7a, should be realized for a high attraction strength $U > U^*$. For smaller attraction strength, $U < U^*$, the adsorbed chain will actually be adsorbed in a layer of width D much larger than the potential width B, as shown in Fig. 7b. Since the threshold energy U^* is proportional to the temperature, it follows that at high temperatures it becomes increasingly difficult to confine the chain. In fact, for an ideal chain, with $\nu = 1/2$, the resulting scaling relation for the critical well depth, $U^* \sim k_{\rm B}T(a/D)^2$, agrees with exact transfer-matrix predictions for the adsorption threshold in a square-well potential [23].

We turn now to the case of a weakly adsorbed polymer layer. The potential depth is smaller than the threshold, i.e., $U < U^*$, and the stability of the weakly adsorbed polymer chains (depicted in Fig. 7b) has to be examined. The thickness D of this polymer layer follows from the minimization of the free energy, Eq. (5), with respect to D, where we use the asymptotic form of the surface potential, Eq. (3), for large separations. The result is

$$D \simeq \left(\frac{a^{1/\nu}k_{\rm B}T}{b}\right)^{\nu/(1-\nu\tau)} \tag{6}$$

Under which circumstances is the prediction of Eq. (6) correct, at least on a qualitative level? It turns out that the prediction for D, Eq. (6), obtained within the simple mean-field theory, is correct if the attractive tail of the substrate potential in Eq. (3) decays for large values of z slower than the entropic repulsion in Eq. (4) [24]. In other words, the mean-field theory is valid for weakly adsorbed polymers only for $\tau < 1/\nu$. This can already be guessed from the functional form of the layer thickness, Eq. (6), because for $\tau > 1/\nu$ the layer thickness D goes to zero as b diminishes. Clearly an unphysical result. For ideal polymers (theta solvent, $\nu = 1/2$), the validity condition is $\tau < 2$, whereas for swollen polymers (good solvent conditions, $\nu = 3/5$), it is $\tau < 5/3$. For most interactions (including van der Waals interactions with $\tau = 3$) this condition on τ is not satisfied, and fluctuations are in fact important, as is discussed in the next section.

There are two notable exceptions. The first is for charged polymers close to an oppositely charged surface, in the *absence* of salt ions. Since the attraction of the polymer to an infinite, planar, and charged surface is linear in z, the interaction is described by Eq. (3) with an exponent $\tau = -1$, and the inequality $\tau < 1/\nu$ is satisfied. For charged surfaces, Eq. (6) predicts the thickness D to increase to infinity as the temperature increases or as the attraction strength b (proportional to the surface charge density) decreases. The resulting exponents for the scaling of D follow from Eq. (6) and are $D \sim (T/b)^{1/3}$ for ideal chains, and $D \sim (T/b)^{3/8}$ for swollen chains [25–27].

A second example where the mean-field theory can be used is the adsorption of polyampholytes on charged surfaces [28]. Polyampholytes are polymers consisting of negatively and positively charged monomers. In cases where the total charge on such a polymer adds up to zero, it might seem that the interaction with a charged surface should vanish. However, it turns out that local charge fluctuations

(i.e., local spontaneous dipole moments) lead to a strong attraction of polyampholytes to charged substrates. In the absence of salt this attractive interaction has an algebraic decay with an exponent $\tau = 2$ [28]. On the other hand, in the presence of salt, the effective interaction is exponentially screened, yielding a decay faster than the fluctuation repulsion, Eq. (4). Nevertheless, the mean-field theory, embodied in the free energy expression, Eq. (5), can be used to predict the adsorption phase behavior within the strongly adsorbed case (i.e., far from any desorption transition) [29].

B. Fluctuation Dominated Regime

Here we consider the weakly adsorbed case for substrate potentials which decay (for large separations from the surface) faster than the entropic repulsion, Eq. (4), i.e., $\tau > 1/\nu$. This applies, e.g., to van der Waals attractive interaction between the substrate and monomers, screened electrostatic interactions, or any other short-ranged potential. In this case, fluctuations play a decisive role. In fact, for *ideal chains*, it can be rigorously proven (using transfer-matrix techniques) that all potentials decaying faster than z^{-2} for large z have a continuous adsorption transition at a finite critical temperature T^* [24]. This means that the thickness of the adsorbed polymer layer diverges for $T \to T^*$ as

$$D \sim (T^* - T)^{-1} \tag{7}$$

The power law divergence of D is universal. Namely, it does not depend on the specific functional form and strength of the potential as long as they satisfy the above condition.

The case of *nonideal chains* is much more complicated. First, progress has been made by de Gennes who recognized the analogy between the partition function of a self-avoiding chain and the correlation function of an n-component spin model in the zero-component ($n \to 0$) limit [30]. The adsorption behavior of nonideal chains has been treated by field-theroetical methods using the analogy to surface critical behavior of magnets (again in the $n \to 0$ limit) [6, 31]. The resulting behavior is similar to the ideal-chain case and shows an adsorption transition at a finite temperature, and a continuous increase towards infinite layer thickness characterized by a power law divergence as a function of $T - T^*$ [31].

The complete behavior for ideal and swollen chains can be described using scaling ideas in the following way. The entropic loss due to the confinement of the chain to a region of thickness D close to the surface is again given by Eq. (4). Assuming that the adsorption layer is much thicker than the range of the attractive potential $V(z)$, the attractive potential can be assumed to be localized at the substrate surface $V(z) \simeq V(0)$. The attractive free energy of the chain to the substrate surface can then be written as [32]

$$\mathcal{F}_{\text{att}} \simeq -\tilde{\gamma} k_B (T^* - T) N f_1 = -\gamma_1 a^2 N f_1 \tag{8}$$

where f_1 is the probability of finding a monomer at the substrate surface, and $\tilde{\gamma}$ is a dimensionless interaction parameter. Two surface excess energies are typically being used: $\gamma_1 = \tilde{\gamma} k_B (T^* - T)/a^2$ is the excess of energy per unit area, while $\gamma_1 a^2$ is the excess of energy per monomer at the surface. Both are positive for the attractive case

(adsorption) and negative for the depletion case. The dependence of γ_1 on T in Eq. (8) causes the attraction to vanish at a critical temperature, $T = T^*$, in accord with our expectations.

The contact probability for a swollen chain with the surface, f_1, can be calculated as follows [33]. In order to force the chain of polymerization index N to be in contact with the wall, one of the chain ends is pinned to the substrate. The number of monomers which are in contact with the surface can be calculated using field-theoretical methods and is given by N^{φ}, where φ is called the *surface crossover exponent* [6, 31]. The fraction of bound monomers follows to be $f_1 \sim N^{\varphi - 1}$, and thus goes to zero as the polymer length increases, for $\varphi < 1$. Now instead of speaking of the entire chain, we refer to a "chain of blobs" (see Fig. 7) adsorbing on the surface, each blob consisting of g monomers. We proceed by assuming that the size of an adsorbed blob D scales with the number of monomers per blob g similarly as in the bulk, $D \sim a g^{\nu}$, as is indeed confirmed by field-theoretical calculations. The fraction of bound monomers can be expressed in terms of D and is given by

$$f_1 \sim \left(\frac{D}{a}\right)^{(\varphi - 1)/\nu} \tag{9}$$

Combining the entropic repulsion, Eq. (4), and the substrate attraction, Eqs (8) and (9), the total free energy is given by

$$\frac{\mathcal{F}}{k_B T} \simeq N\left(\frac{a}{D}\right)^{1/\nu} - N\frac{\tilde{\gamma}(T^* - T)}{T}\left(\frac{D}{a}\right)^{(\varphi - 1)/\nu} \tag{10}$$

Minimization with respect to D leads to the final result:

$$D \simeq a\left[\frac{\tilde{\gamma}(T^* - T)}{T}\right]^{-\nu/\varphi} \simeq a\left(\frac{\gamma_1 a^2}{k_B T}\right)^{-\nu/\varphi} \tag{11}$$

For ideal chains, one has $\varphi = \nu = 1/2$, and thus we recover the prediction from the transfer-matrix calculations, Eq. (7). For nonideal chains, the crossover exponent φ is, in general, different from the swelling exponent ν. However, extensive Monte Carlo computer simulations point to a value for φ very close to ν, such that the adsorption exponent ν/φ appearing in Eq. (11) is very close to unity for polymers embedded in three-dimensional space [31].

A further point which has been calculated using field theory is the behavior of the monomer volume fraction $\phi(z)$ close to the substrate. From rather general arguments borrowed from the theory of critical phenomena, one expects a power-law behavior for $\phi(z)$ at sufficiently small distances from the substrate [31, 33, 34]:

$$\phi(z) \simeq \phi_s (z/a)^m \tag{12}$$

recalling that the monomer density is related to $\phi(z)$ by $c(z) = \phi(z)/a^3$.

In the following, we relate the so-called *proximal exponent* m with the two other exponents introduced above, ν and φ. First note that the surface value of the monomer volume fraction, $\phi_s = \phi(z \approx a)$, for one adsorbed blob follows from the number

of monomers at the surface per blob, which is given by $f_1 g$, and the cross-sectional area of a blob, which is of the order of D^2. The surface volume fraction is given by

$$\phi_s \sim \frac{f_1 g a^2}{D^2} \sim g^{\varphi-2\nu} \tag{13}$$

Using the scaling prediction, Eq. (12), we see that the monomer volume fraction at the blob center, $z \simeq D/2$, is given by $\phi(D/2) \sim g^{\varphi-2\nu}(D/a)^m$, which (again using $D \sim ag^\nu$) can be rewritten as $\phi(D/2) \simeq g^{\varphi-2\nu+m\nu}$.

On the other hand, at a distance $D/2$ from the surface, the monomer volume fraction should have decayed to the average monomer volume fraction $a^3 g/D^3 \simeq g^{1-3\nu}$ inside the blob since the statistics of the chain inside the blob is the same for a chain in the bulk. By direct comparison of the two volume fractions, we see that the exponents $\varphi - 2\nu + m\nu$ and $1 - 3\nu$ have to match in order to have a consistent result, yielding

$$m = \frac{1-\varphi-\nu}{\nu} \tag{14}$$

For an ideal chain (theta solvents), one has $\varphi = \nu = 1/2$. Hence, the proximal exponent vanishes, $m = 0$. This means that the proximal exponent has no mean-field analog, explaining why it was discovered only within field-theoretical calculations [6, 31]. In the presence of correlations (good solvent conditions) one has $\varphi \simeq \nu \simeq 3/5$ and thus $m \simeq 1/3$.

Using $D \simeq ag^\nu$ and Eq. (11), the surface volume fraction, Eq. (13), can be rewritten as

$$\phi_s \sim \left(\frac{D}{a}\right)^{(\varphi-2\nu)/\nu} \sim \left(\frac{\gamma_1}{k_B T}\right)^{(2\nu-\varphi)/\varphi} \simeq \frac{\gamma_1}{k_B T} \tag{15}$$

where in the last approximation appearing in Eq. (15) we used the fact that $\varphi \simeq \nu$. The last result shows that the surface volume fraction within one blob can become large if the adsorption energy γ_1 is large enough as compared with $k_B T$. Experimentally, this is very often the case, and additional interactions (such as multibody interactions) between monomers at the surface have, in principle, to be taken into account.

After having discussed the adsorption behavior of a single chain, a word of caution is in order. Experimentally, one never looks at single chains adsorbed to a surface. First, this is because one always works with polymer solutions, where there is a large number of polymer chains contained in the bulk reservoir, even when the bulk monomer (or polymer) concentration is quite low. Second, even if the bulk polymer concentration is very low, and in fact so low that polymers in solution rarely interact with each other, the surface concentration of polymer is enhanced relative to that in the bulk. Therefore, adsorbed polymers at the surface usually do interact with neighboring chains, owing to the higher polymer concentration at the surface [34].

Nevertheless, the adsorption behavior of a single chain serves as a basis and guideline for the more complicated adsorption scenarios involving many-chain effects. It will turn out that the scaling of the adsorption layer thickness D and the proximal volume fraction profile, Eqs (11) and (12), are not affected by the presence of other chains. This finding as well as other many-chain effects on polymer adsorption is the subject of the next section.

III. POLYMER ADSORPTION FROM SOLUTION

A. The Mean-Field Approach: Ground State Dominance

In this section we look at the equilibrium behavior of many chains adsorbing on (or equivalently depleting from) a surface in contact with a bulk reservoir of chains at equilibrium. The polymer chains in the reservoir are assumed to be in a semidilute concentration regime. The semi-dilute regime is defined by $c > c^*$, where c denotes the monomer concentration (per unit volume) and c^* is the concentration where individual chains start to overlap. Clearly, the overlap concentration is reached when the average bulk monomer concentration exceeds the monomer concentration inside a polymer coil. To estimate the overlap concentration c^*, we simply note that the average monomer concentration inside a coil with dimension $R_e \sim aN^\nu$ is given by $c^* \sim N/R_e^3 \sim N^{1-3\nu}/a^3$.

As in the previous section, the adsorbing surface is taken as an ideal and smooth plane. Neglecting lateral concentration fluctuations, one can reduce the problem to an effective one-dimensional problem, where the monomer concentration depends only on the distance z from the surface, $c = c(z)$. The two boundary conditions are: $c_b = c(z \to \infty)$ in the bulk, while $c_s = c(z = 0)$ on the surface.

In addition to the monomer concentration c, it is more convenient to work with the monomer volume fraction: $\phi(z) = a^3 c(z)$ where a is the monomer size. While the bulk value (far away from the surface) is fixed by the concentration in the reservoir, the value on the surface at $z = 0$ is self-adjusting in response to a given surface interaction. The simplest phenomenological surface interaction is linear in the surface polymer concentration. The resulting contribution to the surface free energy (per unit area) is

$$F_s = -\gamma_1 \phi_s \tag{16}$$

where $\phi_s = a^3 c_s$ and a positive (negative) value of $\gamma_1 = \tilde{\gamma} k_B (T - T^*)/a^2$, defined in the previous section, enhances adsorption (depletion) of the chains on (from) the surface. However, F_s represents only the local reduction in the interfacial free energy due to the adsorption. In order to calculate the full interfacial free energy, it is important to note that monomers adsorbing on the surface are connected to other monomers belonging to the same polymer chain. The latter accumulate in the vicinity of the surface. Hence, the interfacial free energy does not only depend on the surface concentration of the monomers but also on their concentration in the *vicinity* of the surface. Due to the polymer flexibility and connectivity, the entire adsorbing layer can have a considerable width. The *total* interfacial free energy of the polymer chains will depend on this width and is quite different from the interfacial free energy for simple molecular liquids.

There are several theoretical approaches for treating this polymer adsorption. One of the simplest approaches which yet gives reasonable qualitative results is that of Cahn–de Gennes [35, 36]. In this approach, it is possible to write down a continuum functional which describes the contribution to the free energy of the polymer chains in the solution. This procedure was introduced by Edwards in the 1960s [15]

and was applied to polymers at interfaces by de Gennes [36]. Below, we present such a continuum version which can be studied analytically. Another approach is a discrete one, where the monomers and solvent molecules are put on a lattice. The latter approach is quite useful in computer simulations and numerical self-consistent field (SCF) studies, and is reviewed elsewhere [5].

In the continuum approach and using a mean-field theory, the bulk contribution to the adsorption free energy is written in terms of the local monomer volume fraction $\phi(z)$, neglecting all kinds of monomer–monomer correlations. The total reduction in the surface tension (interfacial free energy per unit area) is then

$$\gamma - \gamma_0 = -\gamma_1 \phi_s + \int_0^\infty dz \left[L(\phi) \left(\frac{d\phi}{dz} \right)^2 + F(\phi) - F(\phi_b) + \mu(\phi - \phi_b) \right] \tag{17}$$

where γ_0 is the bare surface tension of the surface in contact with the solvent, but without the presence of the monomers in solution, and γ_1 was defined in Eq. (16). The stiffness function $L(\phi)$ represents the energy cost of local concentration fluctuations and its form is specific to long polymer chains. For low polymer concentration it can be written as [11]

$$L(\phi) = \frac{k_B T}{a^3} \left(\frac{a^2}{24\phi} \right) \tag{18}$$

where $k_B T$ is the thermal energy. The other terms in Eq. (17) come from the Cahn–Hilliard free energy of mixing of the polymer solution, μ being the chemical potential, and [8]

$$F(\phi) = \frac{k_B T}{a^3} \left(\frac{\phi}{N} \log \phi + \frac{1}{2} v\phi^2 + \frac{1}{6} w\phi^3 + \cdots \right) \tag{19}$$

where N is the polymerization index. In the following, we neglect the first term in Eq. (19) (translational entropy), as can be justified in the long-chain limit, $N \gg 1$. The second and third dimensionless virial coefficients are v and w, respectively. Good, bad, and theta solvent conditions are achieved, respectively, for positive, negative, or zero v. We concentrate hereafter only on good solvent conditions, $v > 0$, in which case the higher order w term can be safely neglected. In addition, the local monomer density is assumed to be small enough to justify the omission of higher virial coefficients. Note that for small molecules the translational entropy always acts in favor of desorbing from the surface. As was discussed in Section I, the vanishingly small translational entropy for polymers results in a stronger adsorption (as compared with low molecular weight solutes) and makes the polymer adsorption much more of an irreversible process.

The key feature in obtaining Eq. (17) is the so-called *ground state dominance*, where, for long enough chains $N \gg 1$, only the lowest energy eigenstate (ground state) of a diffusion-like equation is taken into account. This approximation gives us the leading behavior in the $N \to \infty$ limit [21]. It is based on the fact that the weight of the first excited eigenstate is smaller than that of the ground state by an exponential factor: $\exp(-N\Delta E)$ where $\Delta E = E_1 - E_0 > 0$ is the difference in the eigenvalues between the two eigenstates. Clearly, close to the surface more details on the polymer conformations can be important. The adsorbing chains have tails (end sections of the chains that are connected to the surface by only one end), loops

(mid-sections of the chains that are connected to the surface by both ends), and trains (sections of the chains that are adsorbed on the surface), as depicted in Fig. 3a. To some extent it is possible to obtain profiles of the various chain segments even within mean-field theory, if the ground state dominance condition is relaxed as is discussed below.

Taking into account all those simplifying assumptions and conditions, the mean-field theory for the interfacial free energy can be written as

$$\gamma - \gamma_0 = -\gamma_1 \phi_s + \frac{k_B T}{a^3} \int_0^\infty dz \left[\frac{a^2}{24\phi} \left(\frac{d\phi}{dz} \right)^2 + \frac{1}{2} v[\phi(z) - \phi_b]^2 \right] \tag{20}$$

where the monomer bulk chemical potential μ is given by $\mu = \partial F / \partial \phi|_b = v\phi_b$.

It is also useful to define the total amount of monomers per unit area which take part in the adsorption layer. This is the so-called surface excess Γ; it is measured experimentally using, e.g., ellipsometry, and is defined as

$$\Gamma = \frac{1}{a^3} \int_0^\infty dz[\phi(z) - \phi_b] \tag{21}$$

The next step is to minimize the free energy functional, Eq. (20), with respect to both $\phi(z)$ and $\phi_s = \phi(0)$. It is more convenient to re-express Eq. (20) in terms of $\psi(z) = \phi^{1/2}(z)$ and $\psi_s = \phi_s^{1/2}$:

$$\gamma - \gamma_0 = -\gamma_1 \psi_s^2 + \frac{k_B T}{a^3} \int_0^\infty dz \left[\frac{a^2}{6} \left(\frac{d\psi}{dz} \right)^2 + \frac{1}{2} v\left[\psi^2(z) - \psi_b^2\right]^2 \right] \tag{22}$$

Minimization of Eq. (22) with respect to $\psi(z)$ and ψ_s leads to the following profile equation and boundary condition:

$$\begin{aligned} &\frac{a^2}{6} \frac{d^2\psi}{dz^2} = v\psi(\psi^2 - \psi_b^2) \\ &\frac{1}{\psi_s} \frac{d\psi}{dz}\bigg|_s = -\frac{6a}{k_B T} \gamma_1 = -\frac{1}{2D} \end{aligned} \tag{23}$$

The second equation sets a boundary condition on the logarithmic derivative of the monomer volume fraction, $d \log \phi / dz|_s = 2\psi^{-1} d\psi/dz|_s = -1/D$, where the strength of the surface interaction γ_1 can be expressed in terms of a length $D \equiv k_B T/(12a\gamma_1)$. Note that exactly the same scaling of D on γ_1/T is obtained in Eq. (11) for the single-chain behavior if one sets $\nu = \varphi = 1/2$ (ideal chain exponents). This is strictly valid at the upper critical dimension ($d = 4$) and is a very good approximation in three dimensions.

The profile equation (23) can be integrated once, yielding

$$\frac{a^2}{6} \left(\frac{d\psi}{dz} \right)^2 = \frac{1}{2} v\left[\psi^2 - \psi_b^2\right]^2 \tag{24}$$

The above differential equation can now be solved analytically. We first present the results in more detail for polymer adsorption ($\gamma_1 > 0$) and then repeat the main findings for polymer depletion ($\gamma_1 < 0$).

1. Polymer Adsorption

Setting $\gamma_1 > 0$ as is applicable for the adsorption case, the first-order differential equation (24) can be integrated and, together with the boundary condition, Eq. (23), yields:

$$\phi(z) = \phi_b \coth^2\left(\frac{z + z_0}{\xi_b}\right) \tag{25}$$

where the length $\xi_b = a/\sqrt{3v\phi_b}$ is the Edwards correlation length characterizing the exponential decay of concentration fluctuations in the bulk [11, 15]. The length z_0 is not an independent length since it depends on D and ξ_b, as can be seen from the boundary condition, Eq. (23):

$$z_0 = \frac{\xi_b}{2}\,\mathrm{arcsinh}\left(\frac{4D}{\xi_b}\right) = \xi_b\,\mathrm{arccoth}\left(\sqrt{\phi_s/\phi_b}\right) \tag{26}$$

Furthermore, ϕ_s can be directly related to the surface interaction γ_1 and the bulk value ϕ_b:

$$\frac{\xi_b}{2D} = \frac{6a^2\gamma_1}{k_B T\sqrt{3v\phi_b}} = \sqrt{\frac{\phi_b}{\phi_s}}\left(\frac{\phi_s}{\phi_b} - 1\right) \tag{27}$$

In order to be consistent with the semidilute concentration regime, the correlation length ξ_b should be smaller than the size of a single chain, $R_e = aN^\nu$, where $\nu \simeq 3/5$ is the Flory exponent in good solvent conditions. This sets a lower bound on the polymer concentration in the bulk, $c > c^*$.

So far, three length scales have been introduced: the Kuhn length or monomer size a, the adsorbed-layer width D, and the bulk correlation length ξ_b. It is more convenient for the discussion to consider the case where those three length scales are quite separate: $a \ll D \ll \xi_b$. Two conditions must be satisfied. On the one hand, the adsorption parameter is not large, $12a^2\gamma_1 \ll k_B T$ in order to have $D \gg a$; on the other, the adsorption energy is large enough to satisfy $12a^2\gamma_1 \gg k_B T\sqrt{3v\phi_b}$ in order to have $D \ll \xi_b$. The latter inequality can also be regarded as a condition for the polymer bulk concentration. The bulk correlation length is large enough if indeed the bulk concentration (assumed to be in the semidilute concentration range) is not too large. Roughly, let us assume in a typical case that the three length scales are well separated: a is of the order of a few angstroms, D of the order of a few dozen angstroms, and ξ_b of the order of a few hundred angstroms.

When the above two inequalities are satisfied, three spatial regions of adsorption can be differentiated: the proximal, central, and distal regions, as is outlined below. In addition, as soon as $\xi_b \gg D$, $z_0 \simeq 2D$, as follows from Eq. (26).

- Close enough to the surface, $z \sim a$, the adsorption profile depends on the details of the short-range interactions between the surface and monomers. Hence, this region is not universal. In the proximal region, for $a \gg z \gg D$, corrections to the mean-field theory analysis (which assumes the concentration to be constant) are presented below similarly to the treatment of the single-chain section. These corrections reveal a new scaling exponent characterizing the concentration profile. They are of particular importance close to the adsorption/desorption transition.

- In the distal region, $z \gg \xi_b$, the excess polymer concentration decays exponentially to its bulk value:

$$\phi(z) - \phi_b \simeq 4\phi_b e^{-2z/\xi_b} \tag{28}$$

  as follows from Eq. (25). This behavior is very similar to the decay of fluctuations in the bulk, with ξ_b being the correlation length.
- Finally, in the central region (and with the assumption that ξ_b is the largest length scale in the problem), $D \ll z \ll \xi_b$, the profile is universal and from Eq. (25) it can be shown to decay with a powere law:

$$\phi(z) = \frac{1}{3v}\left(\frac{a}{z + 2D}\right)^2 \tag{29}$$

A sketch of the different scaling regions in the adsorption profile is given in Fig. 8a. Included in this figure are corrections in the proximal region, which is discussed further below.

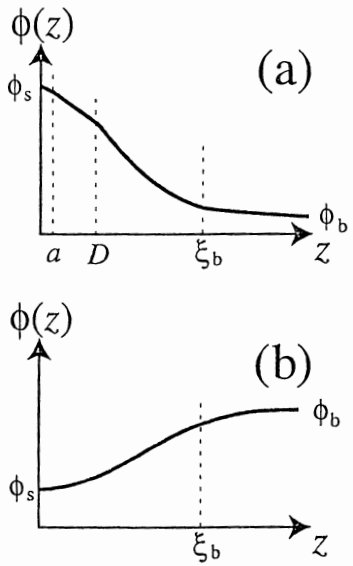

FIG. 8 (a) The schematic density profile for the case of adsorption from a semidilute solution; we distinguish a layer of molecular thickness $z \sim a$ where the polymer density depends on details of the interaction with the substrate and the monomer size, the proximal region $a < z < D$ where the decay of the density is governed by a universal power law (which cannot be obtained within mean-field theory), the central region for $D < z < \xi_b$ with a self-similar profile, and the distal region for $\xi_b < z$, where the polymer concentration relaxes exponentially to the bulk volume fraction ϕ_b. (b) The density profile for the case of depletion, where the concentration decrease close to the wall ϕ_s relaxes to its bulk value ϕ_b at a distance of the order of the bulk correlation length ξ_b.

A special consideration should be given to the formal limit of setting the bulk concentration to zero, $\phi_b \to 0$ (and equivalently $\xi_b \to \infty$), which denotes the limit of an adsorbing layer in contact with a polymer reservoir of vanishing concentration. It should be emphasized that this limit is not consistent with the assumption of a semidilute polymer solution in the bulk. Still, some information on the polymer density profile close to the adsorbing surface, where the polymer solution is locally semidilute [34] can be obtained. Formally, we take the limit $\xi_b \to \infty$ in Eq. (25), and obtain the limiting expression given by Eq. (29), which does not depend on ξ_b. The profile in the central region decays algebraically. In the case of zero polymer concentration in the bulk, the natural cut-off is not ξ_b but rather R_e, the coil size of a single polymer in solution. Hence, the distal region loses its meaning and is replaced by a more complicated scaling regime [37]. The length D can be regarded as the layer thickness in the $\xi_b \to \infty$ limit in the sense that a finite fraction of all the monomers are located in this layer of thickness D from the surface. Another observation is that $\phi(z) \sim 1/z^2$ for $z \gg D$. This power law is a result of the mean-field theory, and its modification is discussed below.

It is now possible to calculate within the mean-field theory the two physical quantities that are measured in many experiments: the surface tension reduction $\gamma - \gamma_0$ and the surface excess Γ.

The surface excess, defined in Eq. (21), can be calculated in a close form by inserting Eq. (25) into Eq. (21),

$$\Gamma = \frac{1}{\sqrt{3v}a^2}(\phi_s^{1/2} - \phi_b^{1/2}) = \frac{\xi_b \phi_b}{a^3}\left(\sqrt{\frac{\phi_s}{\phi_b}} - 1\right) \tag{30}$$

For strong adsorption, we obtain from Eq. (27) that $\phi_s \simeq (a/2D)^2/3v \gg \phi_b$, and Eq. (30) reduces to

$$\Gamma = \frac{1}{3va^2}\left(\frac{a}{D}\right) \sim \gamma_1 \tag{31}$$

while the surface volume fraction scales as $\phi_s \sim \gamma_1^2$. As can be seen from Eqs (31) and (29), the surface excess as well as the entire profile does not depend (to leading order) on the bulk concentration ϕ_b. We note again that the strong adsorption condition is always satisfied in the $\phi_b \to 0$ limit. Hence, Eq. (31) can be obtained directly by integrating the profile in the central region, Eq. (29).

Finally, let us calculate the reduction in surface tension for the adsorbing case. Inserting the variational equations (23) in Eq. (20) yields:

$$\gamma - \gamma_0 = -\gamma_1 \phi_s + \frac{k_B T \sqrt{3v}}{9a^2}\phi_s^{3/2}\left[1 - 3\left(\frac{\phi_b}{\phi_s}\right) + 2\left(\frac{\phi_b}{\phi_s}\right)^{3/2}\right] \tag{32}$$

The surface term in Eq. (32) is negative while the second term is positive. For strong adsorption this reduction of γ does not depend on ϕ_b and reduces to

$$\gamma - \gamma_0 \sim -\left(\frac{\gamma_1 a^2}{k_B T}\right)^3 \frac{k_B T}{a^2} + \mathcal{O}(\gamma_1^{4/3}) \tag{33}$$

where the leading term is just the contribution of the surface monomers.

2. Polymer Depletion

We highlight the main differences between the polymer adsorption and polymer depletion. Keeping in mind that $\gamma_1 < 0$ for depletion, the solution of the same profile equation (24), with the appropriate boundary condition, results in

$$\phi(z) = \phi_b \tanh^2\left(\frac{z + z_0}{\xi_b}\right) \tag{34}$$

which is schematically plotted in Fig. 8b. The limit $\phi_b \to 0$ cannot be taken in the depletion case since depletion with respect to a null reservoir has no meaning. However, we can, alternatively, look at the strong depletion limit, defined by the condition $\phi_s \ll \phi_b$. Here we find

$$\phi(z) = 3v\phi_b^2\left(\frac{z + 2D}{a}\right)^2 \tag{35}$$

In the same limit, we find for the surface volume fraction $\phi_s \sim \phi_b^2 \gamma_1^{-2}$, and the exact expression for the surface excess, Eq. (30), reduces to

$$\Gamma = -\frac{1}{a^2}\sqrt{\frac{\phi_b}{3v}} \simeq -\frac{\phi_b \xi_b}{a^3} \tag{36}$$

The negative surface excess can be directly estimated from a profile varying from ϕ_b to zero over a length scale of order ξ_b.

The dominating behavior for the surface tension can be calculated from Eq. (20) where both terms are now positive. For the strong depletion case we obtain:

$$\gamma - \gamma_0 \simeq \frac{k_B T}{a^2}\left(\frac{a}{\xi_b}\right)^3 \sim \phi_b^{3/2} \tag{37}$$

B. Beyond Mean-Field Theory: Scaling Arguments for Good Solvents

One of the mean-field theory results that should be corrected is the scaling of the correlation length with ϕ_b. In the semidilute regime, the correlation length can be regarded as the average mesh size created by the overlapping chains. It can be estimated using very simple scaling arguments [11]: The volume fraction of monomers inside a coil formed by a subchain consisting of g monomers is $\phi \sim g^{1-3\nu}$ where ν is the Flory exponent. The spatial scale of this subchain is given by $\xi_b \sim a g^{\nu}$. Combining these two relations, and setting $\nu \simeq 3/5$, as appropriate for good solvent conditions, we obtain the known scaling of the correlation length:

$$\xi_b \simeq a\phi_b^{3/4} \tag{38}$$

This relation corrects the mean-field theory result $\xi_b \sim \phi_b^{-1/2}$, which can be obtained from, e.g., Eq. (20).

1. Scaling for Polymer Adsorption

We repeat here an argument due to de Gennes [36]. The main idea is to assume that the relation Eq. (38) holds locally: $\phi(z) = [\xi(z)/a]^{-4/3}$, where $\xi(z)$ is the local "mesh size" of the semidilute polymer solution. Since there is no other length scale in the

problem beside the distance from the surface, z, the correlation length $\xi(z)$ should scale as the distance z itself, $\xi(z) \simeq z$, leading to the profile:

$$\phi(z) \simeq \left(\frac{a}{z}\right)^{4/3} \tag{39}$$

We note that this argument holds only in the central region $D \ll z \ll \xi_b$. It has been confirmed experimentally using neutron scattering [38] and neutron reflectivity [39]. Equation (39) satisfies the distal boundary condition: $z \to \xi_b$, $\phi(z) \to \phi_b$, but for $z > \xi_b$ we expect the regular exponential decay behavior of the distal region, Eq. (28). De Gennes also proposed (without a rigorous proof) a convenient expression for $\phi(z)$, which has the correct crossover from the central to the mean-field proximal region [36]:

$$\phi(z) = \phi_s\left(\frac{\frac{4}{3}D}{z+\frac{4}{3}D}\right)^{4/3} \simeq \left(\frac{a}{z+\frac{4}{3}D}\right)^{4/3} \tag{40}$$

Note that the above equation reduces to Eq. (39) for $z \gg D$. The extrapolation of Eq. (40) also gives the correct definition of D: $D^{-1} = -\mathrm{d}\log\phi/\mathrm{d}z|_s$. In addition, ϕ_s is obtained from the extrapolation to $z = 0$ and scales as

$$\phi_s = \phi(z=0) = \left(\frac{a}{D}\right)^{4/3} \tag{41}$$

For strong adsorption ($\phi_s \gg \phi_b$), we have

$$\begin{aligned}
\phi_s &\simeq \left(\frac{a}{D}\right)^{4/3} \sim \gamma_1^2 \\
D &\simeq a\left(\frac{k_B T}{a^2\gamma_1}\right)^{3/2} \sim \gamma_1^{-3/2} \\
\Gamma &\simeq a^2\left(\frac{a^2\gamma_1}{k_B T}\right)^{1/2} \sim \gamma_1^{1/2} \\
\gamma - \gamma_0 &\simeq -\frac{k_B T}{a^2}\phi_s^{3/2} \sim -\gamma_1^3
\end{aligned} \tag{42}$$

It is interesting to note that although D and Γ have different scaling with the surface interaction γ_1 in the mean-field theory and scaling approaches, ϕ_s and $\gamma - \gamma_0$ have the same scaling using both approaches. This is a result of the same scaling $\phi_s \sim \gamma_1^2$, which, in turn, leads to $\gamma - \gamma_0 \simeq \gamma_1\phi_s \sim \gamma_1^3$.

2. Scaling for Polymer Depletion

For polymer depletion, similar arguments [36] suggest the following scaling form for the central and mean-field proximal regions, $a < z < \xi_b$:

$$\phi(z) = \phi_b\left(\frac{z+\frac{5}{3}D}{\xi_b}\right)^{5/3} \tag{43}$$

where the depletion thickness is $\xi_b - D$, whereas in the strong depletion regime ($\phi_s \ll \phi_b$):

$$\begin{aligned}
\phi_s &\simeq \phi_b\left(\frac{D}{\xi_b}\right)^{5/3} \sim \phi_b^{9/4}\gamma_1^{-5/2} \\
D &= a\left(\frac{a^2\gamma_1}{k_B T}\right)^{-3/2} \\
\Gamma &\simeq -\phi_b a^{-3}(\xi_b - D) \sim \phi_b^{1/4} \\
\gamma - \gamma_0 &\simeq -\frac{k_B T}{a^2}\phi_b^{3/2}
\end{aligned} \tag{44}$$

Note that the scaling of the surface excess and surface tension with the bulk concentration ϕ_b is similar to that obtained by the mean-field theory approach in Section III.A.2.

C. Proximal Region Corrections

So far we have not addressed any corrections in the proximal region: $a < z < D$ for the many-chain adsorption. In the mean-field theory picture the profile in the proximal region is featureless and saturates smoothly to its extrapolated surface value, $\phi_s > 0$. However, in relation to surface critical phenomena, which is in particular relevant close to the adsorption–desorption phase transition (the so-called "special" transition), the polymer profile in the proximal region has a scaling form with another exponent m:

$$\phi(z) \simeq \phi_s\left(\frac{a}{z}\right)^m \tag{45}$$

where $m = (1 - \varphi - \nu)/\nu$ is the proximal exponent, Eq. (14). This is similar to the single-chain treatment in Section II.

For good solvents, one has $m \simeq 1/3$, as was derived using analogies with surface critical phenomena, exact enumeration of polymer configurations, and Monte Carlo simulations [31]. It is different from the exponent 4/3 of the central region.

With the proximal region correction, the polymer profile can be written as [33]

$$\phi(z) \simeq \begin{cases} \phi_s & \text{for } 0 < z < a \\ \phi_s\left(\frac{a}{z}\right)^{1/3} & \text{for } a < z < D \\ \phi_s\left(\frac{a}{z}\right)^{1/3}\left(\frac{D}{z+D}\right) & \text{for } D < z < \xi_b \end{cases} \tag{46}$$

where

$$\phi_s = \frac{a}{D} \tag{47}$$

The complete adsorption profile is shown in Fig. 8a. By minimization of the free energy with respect to the layer thickness D it is possible to show that D is proportional to $1/\gamma_1$:

$$D \sim \gamma_1^{-1} \tag{48}$$

in accord with the exact field-theoretical results for a single chain as discussed in Section II.

The surface concentration, surface excess, and surface tension have the following scaling [33]:

$$\phi_s \simeq \frac{a}{D} \sim \gamma_1$$
$$\Gamma \simeq a^{-3} D \left(\frac{a}{D}\right)^{4/3} \sim \gamma_1^{1/3}$$
$$\gamma - \gamma_0 \simeq -\frac{\gamma_1 a^2}{k_B T} \gamma_1 \sim \gamma_1^2 \tag{49}$$

Note the differences in the scaling of the surface tension and surface excess in Eq. (49) as compared with the results obtained with no proximity exponent ($m = 0$) in the previous section, Eq. (42).

At the end of our discussion of polymer adsorption from solutions, we would like to add that for the case of adsorption from dilute solutions, there is an intricate crossover from the single-chain adsorption behavior, as discussed in Section II, to the adsorption from semidilute polymer solutions, as discussed in this section [34]. Since the two-dimensional adsorbed layer has a local polymer concentration higher than that of the bulk, it is possible that the adsorbed layer forms a two-dimensional semidilute state, while the bulk is a truly dilute polymer solution. Only for extremely low bulk concentrations or for very weak adsorption energies has the adsorbed layer a single-chain structure with no chain crossings between different polymer chains.

D. Loops and Tails

It was realized quite some time ago that the so-called central region of an adsorbed polymer layer is characterized by a rather broad distribution of loop and tail sizes [5, 40, 41]. A loop is defined as a chain region located between two points of contact with the adsorbing surface, and a tail is defined as the chain region between the free end and the closest contact point to the surface, while a train denotes a chain section which is tightly bound to the substrate (see Fig. 3a). The relative statistical weight of loops and tails in the adsorbed layer is clearly of importance to applications. For example, it is expected that polymer loops which are bound at both ends to the substrate are more prone than tails to entanglements with free polymers and, thus, lead to enhanced friction effects. It was found in detailed numerical mean-field theory calculations that the external part of the adsorbed layer is dominated by dangling tails, while the inner part is mostly built up by loops [5, 40].

Recently, an analytical theory was formulated which correctly takes into account the separate contributions of loops and tails and which thus goes beyond the *ground state dominance* assumption made in ordinary mean-field theories. The theory predicts that a crossover between tail-dominated and loop-dominated regions occurs at some distance $z^* \simeq aN^{1/(d-1)}$ [42] from the surface, where d is the dimension of the embedding space. It is well known that mean-field theory behavior can be formally obtained by setting the embedding dimensionality equal to the upper critical dimension, which is for self-avoiding polymers given by $d = 4$ [12]. Hence, the above expression predicts a crossover in the adsorption behavior at a distance $z^* \simeq aN^{1/3}$. For good-solvent conditions in three dimensions ($d = 3$), $z^* \simeq aN^{1/2}$.

In both cases, the crossover occurs at a separation much smaller than the size of a free polymer $R_e \sim aN^{\nu}$ where, according to the classical Flory argument [8], $\nu = 3/(d+2)$.

A further rather subtle result of these improved mean-field theories is the occurrence of a depletion hole, i.e., a region at a certain separation from the adsorbing surface where the monomer concentration is smaller than the bulk concentration [42]. This depletion hole results from an interplay between the depletion of free polymers from the adsorbed layer and the slowly decaying density profile resulting from dangling tails. It occurs at a distance from the surface comparable with the radius of gyration of a free polymer, but also shows some dependence on the bulk polymer concentration. These and other effects, related to the occurrence of loops and tails in the adsorbed layer, have been recently reviewed [43].

IV. INTERACTION BETWEEN TWO ADSORBED LAYERS

One of the many applications of polymers lies in their influence on the behavior of colloidal particles suspended in a solvent [10]. If the polymers do not adsorb on the surface of the colloidal particles but are repelled from it, a strong attraction between the particles results from this polymer–particle depletion, and can lead to polymer-induced flocculation [44]. If the polymers adsorb uniformly on the colloidal surface (and under good-solvent conditions), they show the experimentally well-known tendency to stabilize colloids against flocculation, i.e., to hinder the colloidal particles from coming so close that van der Waals attractions will induce binding. We should also mention that, in other applications, adsorbing high molecular weight polymers are used in the opposite sense as flocculants to induce binding between unwanted submicrometer particles, thereby, removing them from the solution. It follows that adsorbing polymers can have different effects on the stability of colloidal particles, depending on the detailed parameters.

Hereafter, we assume the polymers to form an adsorbed layer around the colloidal particles, with a typical thickness much smaller than the particle radius, such that curvature effects can be neglected. In that case, the effective interaction between the colloidal particles with adsorbed polymer layers can be traced back to the interaction energy between two planar substrates covered with polymer adsorption layers. In the case when the approach of the two particles is slow and the adsorbed polymers are in *full equilibrium* with the polymers in solution, the interaction between two opposing adsorbed layers is predominantly attractive [45, 46], mainly because polymers form bridges between the two surfaces. Recently, it has been shown that there is a small repulsive component to the interaction at large separations [47].

The typical equilibration times of polymers are extremely long. This holds in particular for adsorption and desorption processes, and is due to the slow diffusion of polymers and their rather high adsorption energies. Note that the adsorption energy of a polymer can be much higher than $k_B T$ even if the adsorption energy of a single monomer is small since there are typically many monomers of a single chain attached to the surface. Therefore, for the typical time scales of colloid contacts, the adsorbed polymers are not in equilibrium with the polymer solution. This is also true for most of the experiments done with a surface-force apparatus, where two polymer layers adsorbed on crossed mica cylinders are brought into contact.

In all these cases one has a *constrained equilibrium* situation, where the polymer configurations and thus the density profile can adjust only with the constraint that the total adsorbed polymer excess stays constant. This case has been first considered by de Gennes [45] and he found that two fully saturated adsorbed layers will strongly repel each other if the total adsorbed amount of polymer is not allowed to decrease. The repulsion is mostly due to osmotic pressure and originates from the steric interaction between the two opposing adsorption layers. It was experimentally verified in a series of force-microscope experiments on PEO layers in water (which is a good solvent for PEO)[48].

In other experiments, the formation of the adsorbtion layer is stopped before the layer is fully saturated. The resulting adsorption layer is called *undersaturated*. If two of these undersaturated adsorption layers approach each other, a strong attraction develops, which only at smaller separation changes to an osmotic repulsion [49]. The theory developed for such nonequilibrium conditions predicts that any surface excess lower than the one corresponding to full equilibrium will lead to attraction at large separations [50]. Similar mechanisms are also at work in colloidal suspensions, if the total surface available for polymer adsorption is large compared to the total polymer added to the solution. In this case, the adsorption layers are also undersaturated, and the resulting attraction is utilized in the application of polymers as flocculation agents [10].

A distinct mechanism, which also leads to attractive forces between adsorption layers, was investigated in experiments with dilute polymer solutions in bad solvents. An example is given by PS in cyclohexane below the theta temperature [51]. The subsequently developed theory [52] showed that the adsorption layers attract each other since the local concentration in the outer part of the adsorption layers is enhanced over the dilute solution and lies in the unstable two-phase region of the bulk phase diagram. Similar experiments were repeated at the theta temperature [53].

The force apparatus was also used to measure the interaction between depletion layers [54], as realized with PS in toluene, which is a good solvent for PS but does not favor the adsorption of PS on mica. Surprisingly, the resultant depletion force is too weak to be detected.

The various regimes and effects obtained for the interaction of polymer solutions between two surfaces have recently been reviewed [55]. It transpires that force-microscope experiments done on adsorbed polymer layers form an ideal tool for investigating the basic mechanisms of polymer adsorption, colloidal stabilization, and flocculation.

V. ADSORPTION OF POLYELECTROLYTES

Adsorption of charged chains (polyelectrolytes) on to charged surfaces is a difficult problem, which is only partially understood from a fundamental point of view. This is the case in spite of the prime importance of polyelectrolyte adsorption in many applications [5]. We comment here briefly on the additional features that are characteristic for the adsorption of charged polymers on surfaces.

A polyelectrolyte is a polymer where a fraction f of its monomers are charged. When the fraction is small, $f \ll 1$, the polyelectrolyte is weakly charged, whereas when f is close to unity, the polyelectrolyte is strongly charged. There are two

common ways to control f [56]. One way is to polymerize a heteropolymer using charged and neutral monomers as building blocks. The charge distribution along the chain is quenched ("frozen") during the polymerization stage, and it is characterized by the fraction of charged monomers on the chain, f. In the second way, the polyelectrolyte is a weak polyacid or polybase. The effective charge of each monomer is controlled by the pH of the solution. Moreover, this annealed fraction depends on the local electric potential. This is in particular important to adsorption processes since the local electric field close to a strongly charged surface can be very different from its value in the bulk solution.

Electrostatic interactions play a crucial role in the adsorption of polyelectrolytes [5, 57, 58]. Besides the fraction f of charged monomers, the important parameters are the surface charge density (or surface potential in the case of conducting surfaces), the amount of salt (ionic strength of low molecular weight electrolyte) in solution, and, in some cases, the solution pH. For polyelectrolytes the electrostatic interactions between the monomers themselves (same charges) are always repulsive, leading to an effective stiffening of the chain [59, 60]. Hence, this interaction will *favor* the adsorption of single polymer chains, since their configurations are already rather extended [61], but it will *oppose* the formation of dense adsorption layers close to the surface [62]. A special case is that of *polyampholytes*, where the charge groups on the chain can be positive as well as negative, resulting in a complicated interplay of attraction and repulsion between the monomers [28, 29]. If the polyelectrolyte chains and the surface are oppositely charged, the electrostatic interactions between them will *enhance* the adsorption.

The role of the salt can be conveniently expressed in terms of the Debye–Hückel screening length, defined as

$$\lambda_{DH} = \left(\frac{8\pi c_{salt} e^2}{\varepsilon k_B T} \right)^{-1/2} \tag{50}$$

where c_{salt} is the concentration of monovalent salt ions, e is the electronic charge, and $\varepsilon \simeq 80$ is the dielectric constant of the water. Qualitatively, the presence of small positive and negative ions at thermodynamical equilibrium screens the r^{-1} electrostatic potential at distances $r > \lambda_{DH}$, and roughly changes its form to $r^{-1} \exp(-r/\lambda_{DH})$. For polyelectrolyte adsorption, the presence of salt has a complex effect. It simultaneously screens the monomer–monomer repulsive interactions as well as the attractive interactions between the oppositely charged surface and polymer.

Two limiting adsorbing cases can be discussed separately:

1. A noncharged surface on which the chains tend to adsorb. Here, the interaction between the surface and the chain does not have an electrostatic component. However, as the salt screens the monomer–monomer electrostatic repulsion, it leads to enhancement of the adsorption.
2. The surface is charged but does not interact with the polymer besides the electrostatic interaction. This is called the pure electrosorption case. At low salt concentration, the polymer charge completely compensates the surface charge. At high salt concentration some of the compensation is done by the salt, leading to a decrease in the amount of adsorbed polymer.

In practice, electrostatic and other types of interactions with the surface can occur in parallel, making the analysis more complex. An interesting phenomenon of *overcompensation* of surface charges by the polyelectrolyte chains is observed, where the chains form a condensed layer and reverse the sign of the total surface charge. This is used, e.g., to build a multilayered structure of cationic and anionic polyelectrolytes – a process that can be continued for a few dozen or even a few hundred times [63–65]. The phenomenon of overcompensation is discussed in Refs 62 and 66, but is still not very well understood.

Adsorption of polyelectrolytes from semidilute solutions is treated either in terms of a discrete multi-Stern layer model [5, 67, 68] or in a continuum approach [62, 69, 70]. In the latter approach, the concentration of polyelectrolytes as well as the electric potential close to the substrate are considered as continuous functions. Both the polymer chains and the electrostatic degrees of freedom are treated on a mean-field theory level. In some cases the salt concentration is considered explicitly [62, 70], while in other works (e.g., [69]) it induces a screened Coulombic interaction between the monomers and the substrate.

In a recent work [62], a simple theory has been proposed to treat polyelectrolyte adsorption from a semidilute bulk. The surface was treated as a surface with constant electric potential. (Note that, in other works, the surface is considered to have a constant charge density.) In addition, the substrate is assumed to be impenetrable by the requirement that the polymer concentration at the wall is zero.

Within a mean-field theory it is possible to write down the coupled profile equations of the polyelectrolyte concentration and electric field, close to the surface, assuming that the small counterions (and salt) concentration obeys a Boltzmann distribution. From numerical solutions of the profile equations as well as scaling arguments the following picture emerges. For very low salt concentration, the surface excess of the polymers Γ and the adsorbed layer thickness D are decreasing functions of f : $\Gamma \sim D \sim f^{-1/2}$. This effect arises from a delicate competition between an enhanced attraction to the substrate, on one hand, and an enhanced electrostatic repulsion between monomers, on the other.

Added salt will screen both the electrostatic repulsion between monomers and the attraction to the surface. In the presence of salt, for low f, Γ scales as $f/c_{\text{salt}}^{1/2}$ until it reaches a maximum value at $f^* \sim (c_{\text{salt}}v)^{1/2}$, v being the excluded volume parameter of the monomers. At this special value, $f = f^*$, the electrostatic contribution to the monomer–monomer excluded volume $v_{\text{el}} \sim f^2\lambda_{\text{DH}}^2$ is exactly equal to the non electrostatic v. For $f > f^*$, $v_{\text{el}} > v$ and the surface excess is a descending function of f, because of the dominance of monomer–monomer electrostatic repulsion. It scales as $c_{\text{salt}}^{1/2}/f$. Chapter 7 of Ref. 5 contains a fair amount of experimental results on polyelectrolyte adsorption.

VI. POLYMER ADSORPTION ON HETEROGENEOUS SURFACES

Polymer adsorption can be coupled in a subtle way with lateral changes in the chemical composition or density of the surface. Such a surface undergoing lateral rearrangements at thermodynamical equilibrium is called an *annealed* surface [71, 72]. A Langmuir monolayer of insoluble surfactant monolayers at the air/water interface is an example of such an annealed surface. As a function of the temperature change, a Langmuir monolayer can undergo a phase transition from a high-temperature homogeneous state to a low-temperature demixed state, where dilute and dense phases coexist. Alternatively, the transition from a dilute phase to a dense one may be induced by compressing the monolayer at constant temperature, in which case the adsorbed polymer layer contributes to the pressure [73]. The domain boundary between the dilute and dense phases can act as a nucleation site for adsorption of bulky molecules [74].

The case where the insoluble surfactant monolayer interacts with a semidilute polymer solution solubilized in the water subphase was considered in some detail. The phase diagrams of the mixed surfactant/polymer system were investigated within the framework of mean-field theory [75]. The polymer enhances the fluctuations of the monolayer and induces an upward shift of the critical temperature. The critical concentration is increased if the monomers are more attracted (or at least less repelled) by the surfactant molecules than by the bare water/air interface. In the case where the monomers are repelled by the bare interface but attracted by the surfactant molecules (or vice versa), the phase diagram may have a triple point. The location of the polymer desorption transition line (i.e., where the substrate–polymer interaction changes from being repulsive to being attractive) appears to have a great effect on the phase diagram of the surfactant monolayer.

VII. POLYMER ADSORPTION ON CURVED INTERFACES AND FLUCTUATING MEMBRANES

The adsorption of polymers on rough substrates is of much interest in applications. One example is the reinforcement of rubbers by filler particles such as carbon black or silica particles [76]. Theoretical models considered sinusoidal surfaces [77] and rough and corrugated substrates [78, 79]. In all cases, enhanced adsorption was found and rationalized in terms of the excess surface available for adsorption.

The adsorption on macroscopically curved bodies leads to slightly modified adsorption profiles, and also to contribution to the elastic bending moduli of the adsorbing surfaces. The elastic energy of liquid-like membrane can be expressed in terms of two bending moduli, κ and κ_G. The elastic energy (per unit area) is

$$\frac{\kappa}{2}(c_1 + c_2)^2 + \kappa_G c_1 c_2 \tag{51}$$

where κ and κ_G are the elastic bending modulus and the Gaussian bending modulus, respectively. The reciprocals of the principal radii of curvature of the surface are given by c_1 and c_2. Quite generally, the effective κ_G turns out to be positive and thus favors the formation of surfaces with negative Gaussian curvature, as, for example, an "egg-carton" structure consisting of many saddles. On the other hand, the effective κ is reduced, leading to a more deformable and flexible surface due to the adsorbed polymer layer [71, 80].

Of particular interest is the adsorption of strongly charged polymers on oppositely charged spheres, because this is a geometry encountered in many collodial science applications and in molecular biology as well [81–85].

In other works, the effects of a modified architecture of the polymers on the adsorption behavior was considered. For example, the adsorption of star polymers [86] and random copolymers [87] was considered.

Note that some polymers exhibit a transition into a glassy state in concentrated adsorbed layers. This glassy state depends on the details of the molecular interaction, which are not considered here. It should be kept in mind that such high-concentration effects can slow down the dynamics of adsorption considerably and will prolong the reach of equilibrium.

VIII. TERMINALLY ATTACHED CHAINS

The discussion has so far assumed that all monomers of a polymer are alike and therefore show the same tendency to adsorb to the substrate surface. For industrial and technological applications, one is often interested in *end-functionalized polymers*. These are polymers which attach with one end only to the substrate, as is depicted in Fig. 3b, while the rest of the polymer is not particularly attracted to (or even repelled from) the grafting surface. Hence, it attains a random-coil structure in the vicinity of the surface. Another possibility of block copolymer grafting (Fig. 3c) will be also briefly discussed.

The motivation to study such terminally attached polymers lies in their enhanced power to stabilize particles and surfaces against flocculation. Attaching a polymer by one end to the surface opens up a much more effective route to stable surfaces. Bridging and creation of polymer loops on the same surface, as encountered in the case of homopolymer adsorption, do not occur if the main-polymer section is chosen such that it does not adsorb to the surface.

Experimentally, the end-adsorbed polymer layer can be built in several different ways, depending on the application in mind. First, one of the polymer ends can be *chemically* bound to the grafting surface, leading to a tight and irreversible attachment [88], shown schematically in Fig. 3b. The second possibility consists of *physical* adsorption of a specialized end-group which favors interaction with the substrate. For example, PS chains have been used which contain a zwitterionic end group that adsorbs strongly on mica sheets [89].

Physical grafting is also possible with a suitably chosen diblock copolymer (Fig. 3c), e.g., a PS–PVP diblock in the solvent toluene at a quartz substrate [90]. Toluene is a *selective solvent* for this diblock, i.e., the PVP [poly(vinylpyridine)] block is strongly adsorbed to the quartz substrate and forms a collapsed anchor, while the PS block is under good-solvent conditions, not adsorbing to the substrate and thus extending into the solvent. General adsorption scenarios for diblock copolymers have been theoretically discussed, both for selective and nonselective solvents [91]. Special consideration has been given to the case when the asymmetry of the diblock copolymer, i.e., the length difference between the two blocks, decreases [91].

Yet another experimental realization of grafted polymer layers is possible with diblock copolymers which are anchored at the liquid–air [92] or at a liquid–liquid interface between two immiscible liquids [93]; this scenario offers the advantage that the surface pressure can be directly measured. A well studied example is a diblock copolymer of PS–PEO. The PS block is shorter and functions as the anchor at the air–water interface as it is not miscible in water. The PEO block is miscible in water, but because of attractive interaction with the air–water interface it forms a quasi-two dimensional layer at very low surface coverage. As the pressure increases and the area per polymer decreases, the PEO block is expelled from the surface and forms a quasi-polymer brush.

In the following we simplify the discussion by assuming the polymers to be irreversibly grafted at one end to the substrate. Let us consider the good-solvent case in the absence of any polymer attraction to the surface. The important new parameter that enters the discussion is the grafting density (or area per chain) σ, which is the inverse of the average area that is available for each polymer at the grafting surface. For small grafting densities, $\sigma < \sigma^*$, the polymers will be far apart from each other and hardly interact, as schematically shown in Fig. 9a. The overlap grafting density is $\sigma^* \sim a^{-2}N^{-6/5}$ for swollen chains, where N is the polymerization index [94].

For large grafting densities, $\sigma > \sigma^*$, the chains overlap. Since we assume the solvent to be good, monomers repel each other. The lateral separation between the polymer coils is fixed by the grafting density, so that the polymers stretch away from the grafting surface in order to avoid each other, as depicted in Fig. 9b. The resulting structure is called a polymer "brush", with a vertical height h which greatly exceeds the unperturbed coil radius [94, 95]. Similar stretched structures occur in many other situations, such as diblock copolymer melts in the strong segregation regime, or polymer stars under good-solvent conditions [96]. The universal occurrence of stretched polymer configurations in many seemingly disconnected situations warrants a detailed discussion of the effects obtained with such systems.

A. Grafted Polymer Layer: A Mean-Field Theory Description

The scaling behavior of the polymer height can be analyzed by using a Flory-like mean-field theory, which is a simplified version of the original Alexander theory [95].

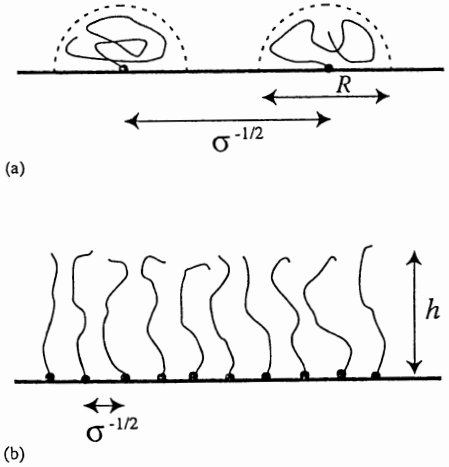

FIG. 9 For grafted chains, one distinguishes (a) the mushroom regime, where the distance between chains, $\sigma^{-1/2}$, is larger than the size of a polymer coil, and (b) the brush regime, where the distance between chains is smaller than the unperturbed coil size. Here, the chains are stretched away from the wall due to repulsive interactions between monomers. The brush height h scales linearly with the polymerization index, $h \sim N$, and is thus larger than the unperturbed coil radius $R_e \sim aN^{\nu}$.

The stretching of the chain leads to an entropic free energy loss of $h^2/(a^2N)$ per chain, and the repulsive energy density resulting from unfavorable monomer–monomer contacts is proportional to the squared monomer density times the dimensionless excluded-volume parameter v (introduced in Section III). The free energy per chain is then

$$\frac{\mathcal{F}}{k_B T} = \frac{3h^2}{2a^2N} + 2a^3 v\left(\frac{\sigma N}{h}\right)^2 \frac{h}{\sigma} \tag{52}$$

where the numerical prefactors were chosen for convenience. The equilibrium height is obtained by minimizing Eq. (52) with respect to h, and the result is [95]

$$h = N(2va^5\sigma/3)^{1/3} \tag{53}$$

The vertical size of the brush scales linearly with the polymerization index N, a clear signature of the strong stretching of the polymer chains. At the overlap threshold, $\sigma^* \sim N^{-6/5}$, the height scales as $h \sim N^{3/5}$, and thus agrees with the scaling of an unperturbed chain radius in a good solvent, as it should. The simple scaling calculation predicts the brush height h correctly in the asymptotic limit of long chains and strong overlap. It has been confirmed by experiments [88–90] and computer simulations [97, 98].

The above scaling result assumes that all chains are stretched to exactly the same height, leading to a step-like shape of the density profile. Monte Carlo and numerical mean-field calculations confirm the general scaling of the brush height, but exhibit a more rounded monomer density profile which goes continuously to zero at the outer perimeter [97]. A large step towards a better understanding of stretched polymer systems was made by Semenov [99], who recognized the importance of *classical paths* for such systems.

The classical polymer path is defined as the path which minimizes the free energy, for a given start and end position, and thus corresponds to the most likely path a polymer takes. The name follows from the analogy with quantum mechanics, where the classical motion of a particle is given by the quantum path with maximal probability. Since for strongly stretched polymers the fluctuations around the classical path are weak, it is expected that a theory which takes into account only classical paths is a good approximation in the strong-stretching limit. To quantify the stretching of the brush, let us introduce the (dimensionless) stretching parameter β, defined as

$$\beta \equiv N\left(\frac{3v^2\sigma^2a^4}{2}\right)^{1/3} = \frac{3}{2}\left(\frac{h}{aN^{1/2}}\right)^2 \tag{54}$$

where $h \equiv N(2v\sigma a^5/3)^{1/3}$ is the brush height according to Alexander's theory [cf. Eq. (53)]. The parameter β is proportional to the square of the ratio of the Alexander prediction for the brush height h and the unperturbed chain radius $R_0 \sim aN^{1/2}$, and, therefore, is a measure of the stretching of the brush. Constructing a classical theory in the infinite-stretching limit, defined as the limit $\beta \to \infty$, it was shown independently by Milner et al. [100] and Skvortsov et al. [101] that the resulting normalized

monomer volume-fraction profile only depends on the vertical distance from the grafting surface. It has in fact a *parabolic* profile given by

$$\phi(z) = \left(\frac{3\pi}{4}\right)^{2/3} - \left(\frac{\pi z}{2h}\right)^2 \tag{55}$$

The brush height, i.e., the value of z for which the monomer density becomes zero, is given by $z^* = (6/\pi^2)^{1/3}h$. The parabolic brush profile has subsequently been confirmed in computer simulations [97, 98] and experiments [88] as the limiting density profile in the strong-stretching limit, and constitutes one of the cornerstones in this field. Intimately connected with the density profile is the distribution of *polymer endpoints*, which is nonzero everywhere inside the brush, in contrast with the original scaling description leading to Eq. (53).

However, deviations from the parablic profile become progressively important as the length of the polymers N or the grafting density σ decreases. In a systematic derivation of the mean-field theory for Gaussian brushes [102] it was shown that the theory is characterized by a single parameter, namely, the stretching parameter β. In the limit $\beta \to \infty$, the difference between the classical approximation and the mean-field theory vanishes, and one obtains the parabolic density profile. For finite β the full mean-field theory and the classical approximation lead to different results and both show deviations from the parabolic profile.

In Fig. 10 we show the density profiles for four different values of β, obtained with the full mean-field theory [102]. The parameter values used are $\beta = 100$ (solid line), $\beta = 10$ (broken line), $\beta = 1$ (dotted–dashed line), and $\beta = 0.1$ (dotted line). For comparison, we also show the asymptotic result according to Eq. (55) as a thick dashed line. In contrast to earlier numerical implementations [5], the self-consistent mean-field equations were solved in the continuum limit, in which case the results only depend on the single parameter β, and direct comparison with other continuum theories becomes possible. Already for $\beta = 100$ the density profile obtained within

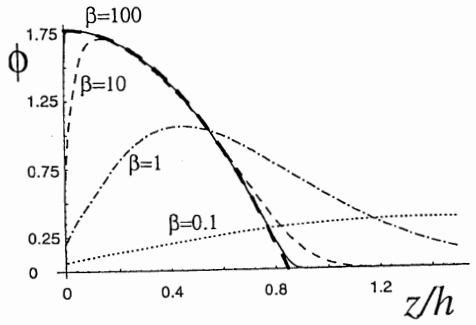

FIG. 10 Results for the density profile of a strongly compressed brush, as obtained within a mean-field theory calculation. As the compression increases, described by the stretching parameter β, which varies from 0.1 (dots) to 1 (dash–dots), 10 (dashes), and 100 (solid line), the density profile approaches the parabolic profile (shown as a thick, dashed line) obtained within a classical-path analysis. (Adapted from Ref. 102.)

mean-field theory is almost indistinguishable from the parabolic profile denoted by a thick dashed line.

Experimentally, the highest values of β achievable are in the range of $\beta \simeq 20$, and therefore deviations from the asymptotic parabolic profile are important. For moderately large values of $\beta > 10$, the classical approximation (not shown here), derived from the mean-field theory by taking into account only one polymer path per end-point position, is still a good approximation, as judged by comparing density profiles obtained from both theories [102], except very close to the surface. The classical theory misses completely the depletion effects at the substrate, which mean-field theory correctly takes into account. Depletion effects at the substrate lead to a pronounced density depression close to the grafting surface, as is clearly visible in Fig. 10.

A further interesting question concerns the behavior of individual polymer paths. As we already discussed for the infinite-stretching theories ($\beta \to \infty$), there are polymer paths ending at any distance from the surface. Analyzing the paths of polymers which end at a common distance from the wall, two rather unexpected features are obtained: (1) free polymer ends are in general stretched, and (2) the end-points lying close to the substrate are pointing towards the surface (such that the polymer paths first move away from the grafting surface before moving towards the substrate), and end-points lying beyond a certain distance from the substrate point away from the surface (such that the paths move monotonically towards the surface). We should point out that these two features have recently been confirmed in molecular-dynamics simulations [103]. They are neither an artifact of the continuous self-consistent theory used in Ref. 102 nor are they due to the neglect of fluctuations. These are interesting results, especially since it has been long assumed that free polymer ends are unstretched, based on the assumption that no forces act on free polymer ends.

Let us now turn to the thermodynamic behavior of a polymer brush. Using the Alexander description, we can calculate the free energy per chain by putting the result for the optimal brush height, Eq. (53), into the free-energy expression, Eq. (52). The result is

$$\mathcal{F}/k_B T \sim N(v\sigma a^2)^{2/3} \tag{56}$$

In the presence of excluded-volume correlations, i.e., when the chain overlap is rather moderate, the brush height h is still correctly predicted by the Alexander calculation, but the prediction for the free energy is in error. Including correlations [95], the free energy is predicted to scale as $\mathcal{F}/k_B T \sim N\sigma^{5/6}$. The osmotic surface pressure Π is related to the free energy per chain by

$$\Pi = \sigma^2 \frac{\partial \mathcal{F}}{\partial \sigma} \tag{57}$$

and should thus scale as $\Pi \sim \sigma^{5/3}$ in the absence of correlations and as $\Pi \sim \sigma^{11/6}$ in the presence of correlations. However, these theoretical predictions do not compare well with experimental results for the surface pressure of a compressed brush [92]. At present, there is no explanation for this discrepancy. An alternative theoretical method for studying tethered chains is the so-called single-chain mean-field method [104], where the statistical mechanics of a single chain is treated exactly, and the interactions with the other chains are taken into account on a mean-field level. This method is especially useful for short chains, where fluctuation effects are important, and dense systems, where excluded-volume interactions play a role. The calculated profiles and brush heights agree very well with those of experiments and computer simulations, and moreover explain the pressure isotherms measured experimentally [92] and in molecular-dynamics simulations [105].

As we described earlier, the main interest in end-adsorbed or grafted polymer layers stems from their ability to stabilize surfaces against van der Waals' attraction. The force between colloids with grafted polymers is repulsive if the polymers do not adsorb on the grafting substrates [106]. This is in accord with our discussion of the interaction between adsorption layers, where attraction was found to be mainly caused by bridging and creation of polymer loops, which of course is absent for nonadsorbing brushes. A stringent test of brush theories was possible with accurate experimental measurements of the repulsive interaction between two opposing grafted polymer layers by using a surface-force apparatus [89]. The resultant force could be fitted very nicely by the infinite-stretching theory of Milner [107]. It was also shown that polydispersity effects, although rather small experimentally, have to be taken into account theoretically in order to obtain a good fit of the data [108].

B. Solvent, Substrate, and Charge Effects on Polymer Grafting

So far we have assumed that the polymer grafted layer is in contact with a good solvent. In this case, the grafted polymers try to minimize their contacts by stretching out into the solvent. If the solvent is bad, the monomers try to avoid the solvent by forming a collapsed brush, the height of which is considerably reduced with respect to the good-solvent case. It turns out that the collapse transition, which leads to phase separation in the bulk, is smeared out for the grafted layer and does not correspond to a true phase transition [109]. The height of the collapsed layer scales linearly in σN, which reflects the constant density within the brush, in agreement with experiments [110]. Some interesting effects have been described theoretically [111] and experimentally [110] for brushes in mixtures of good and bad solvents, and can be rationalized in terms of a partial solvent demixing.

For a theta solvent ($T = T_\theta$) the relevant interaction is described by the third-virial coefficient; using a simple Alexander approach similar to the one leading to Eq. (53), the brush height is predicted to vary with the grafting density as $h \sim \sigma^{1/2}$, in agreement with computer simulations [112].

Up to now we have discussed planar grafting layers. Typically, however, polymers are grafted to curved surfaces. The first study taking into account curvature effects of stretched and tethered polymers was done in the context of star polymers [113]. It was found that chain tethering in the spherical geometry leads to a universal density profile, showing a densely packed core, an intermediate region where correlation effects are negligible and the density decays as $\phi(r) \sim 1/r$, and an outside region where correlations are important and the density decays as $\phi \sim r^{-4/3}$. These considerations were extended using the infinite-stretching theory by Ball et al. [114], self-conistent mean-field theories [115], and molecular-dynamics simulations [116]. Of particular interest is the behavior of the bending rigidity of a polymer brush, which can be calculated from the free energy of a cylindrical and a spherical brush and forms a conceptually simple model for the bending rigidity of a lipid bilayer [117].

A different scenario is obtained with special functionalized lipids with attached water-soluble polymers. If such lipids are incorporated into lipid vesicles, the water-soluble polymers [typically one uses PEG (polyethylene glycol) for its nontoxic properties] form well-separated mushrooms, or, at higher concentration of PEG lipid, a dense brush. These modified vesicles are very interesting in the context of drug delivery, because they show prolonged circulation times in vivo [118]. This is probably the result of steric serum protein-binding inhibition due to the hydrophilic brush coat provided by the PEG lipids. Since the lipid bilayer is rather flexible and undergoes thermal bending fluctuations, there is an interesting coupling between the polymer density distribution and the membrane shape [119]. For nonadsorbing, anchored polymers, the membrane will bend away from the polymer due to steric repulsion, but for adsorbing anchored polymers the membrane will bend towards the polymer [119].

The behavior of a polymer brush in contact with a solvent, which is by itself also a polymer, consisting of chemically identical but somewhat shorter chains than the brush, had been first considered by de Gennes [94]. A complete scaling description has been given only recently [120]. One distinguishes different regimes where the polymer solvent is expelled to various degrees from the brush. A somewhat related question concerns the behavior of two opposing brushes in a solvent which consists of a polymer solution [121]. Here one distinguishes a regime where the polymer solution leads to a strong attraction between the surfaces via the ordinary depletion interaction (cf. [44]), but also a high polymer concentration regime where the attraction is not strong enough to induce colloidal flocculation. This phenomenon is called colloidal restabilization [121].

Another important extension of the brush theory is obtained with charged polymers [122], showing an interesting interplay of electrostatic interactions, polymer elasticity, and monomer–monomer repulsion. Considering a mixed brush made of mutually incompatible grafted chains, a novel transition to a brush characterized by a lateral composition modulation was found [123]. Even more complicated spatial structures are obtained with grafted diblock copolymers [124]. Finally, we would like to mention in passing that these static brush phenomena have interesting consequences on the dynamic properties of polymer brushes [125].

IX. CONCLUDING REMARKS

We have reviewed simple physical concepts underlying the main theories which deal with equilibrium and static properties of polymers adsorbed or grafted to substrates. Most of the review dealt with somewhat ideal situations: smooth and flat surfaces which are chemically homogeneous; long and linear homopolymer chains on which chemical properties can be averaged; and simple phenomenological types of interactions between the monomers and the substrate as well as between the monomers and the solvent.

Even with all the simplifying assumptions, the emerging physical picture is quite rich and robust. Adsorption of polymers from dilute solutions can be understood in terms of a single-chain adsorption on the substrate. Mean-field theory is quite successful, but in some cases fluctations in the local monomer concentration play an important role. Adsorption from more concentrated solutions offers rather complex and rich density profiles, with several regimes (proximal, central, distal).

Each regime is characterized by a different physical behavior. We have reviewed the principal theories used to model the polymer behavior. We also mentioned briefly more recent ideas about the statistics of polymer loops and tails.

The second part of this review was about polymers which are terminally grafted on one end to the surface and are called polymer brushes. The theories here are quite different since the statistics of the grafted layer depend crucially on the fact that the chain is not attracted to the surface but is forced to be in contact with the surface since one of its ends is chemically or physically bonded to the surface. Here as well we reviewed the classical mean-field theory and more advanced theories giving the concentration profiles of the entire polymer layer as well as that of the polymer free ends.

We also discussed additional factors that have an effect on the polymer adsorption and grafted layers: the quality of the solvent, undulating and flexible substrates such as fluid/fluid interfaces or lipid membranes; adsorption and grafted layer of charged polymers (polyelectrolytes); and adsorption and grafting on curved surfaces such as spherical colloidal particles.

Although our main aim was to review the theoretical progress in this field, we mentioned many relevant experiments. In this active field several advanced experimental techniques are used to probe adsorbed or grafted polymer layers: neutron scattering, small-angle high-resolution X-ray scattering, light scattering using fluorescent probes, ellipsometry, and surface isotherms as well as use of the surface-force apparatus to measure forces between two surfaces.

The aim of this chapter was to review the wealth of knowledge on how flexible macromolecules such as linear polymer chains behave as they are adsorbed or grafted to a surface (like an oxide). This chapter should be viewed as a general introduction to these phenomena. Although the chapter does not offer any details about specific oxide/polymer systems, it can serve as a starting point to understanding more complex systems such as encountered in applications and real-life experiments.

ACKNOWLEDGMENTS

We would like to thank I. Borukhov and H. Diamant for discussions and comments. One of us (DA) would like to acknowledge partial support from the Israel Science Foundation founded by the Israel Academy of Sciences and Humanities – Centers of Excellence Program, the Israel–US Binational Science Foundation (BSF) under grant no. 98-00429, and the Tel Aviv University Basic Research Fund. This work was completed during a visit by both of us to the Institute for Theoretical Physics, University of California, Santa Barbara (UCSB).

REFERENCES

1. MA Cohen Stuart, T Cosgrove, B Vincent. Adv Colloid Interface Sci 24:143–239, 1986.
2. PG de Gennes. Adv Colloid Interface Sci 27:189–209, 1987.
3. I Szleifer. Curr Opin Colloid Interface Sci 1:416–423, 1996.
4. GJ Fleer, FAM Leermakers. Curr Opin Colloid Interface Sci 2:308–314, 1997.
5. GJ Fleer, MA Cohen Stuart, JMHM Scheutjens, T Cosgrove, B Vincent. Polymers at Interfaces. London: Chapman & Hall, 1993.
6. E Eisenriegler. Polymers near Surfaces. Singapore: World Scientific, 1993.

7. AYu Grosberg, AR Khokhlov. Statistical Physics of Macromolecules. New York: AIP Press, 1994.
8. PJ Flory. Principles of Polymer Chemistry. Ithaca, NY: Cornell University, 1953.
9. H Yamakawa. Modern Theory of Polymer Solutions. New York: Harper & Row, 1971.
10. DH Napper. Polymeric Stabilization of Colloidal Dispersions. London: Academic Press, 1983.
11. PG de Gennes. Scaling Concepts in Polymer Physics. Ithaca, NY: Cornell University, 1979.
12. J des Cloizeaux, J Jannink. Polymers in Solution. Oxford: Oxford University, 1990.
13. HL Frish, R Simha, FR Eirish. J Chem Phys 21:365, 1953; R Simha, HL Frish, FR Eirish. J Phys Chem 57:584, 1953.
14. A Silberberg. J Phys Chem 66:1872, 1962; 66:1884, 1962.
15. SF Edwards. Proc Phys Soc (London) 85:613, 1965; 88:265, 1966.
16. EA DiMarzio. J Chem Phys 42:2101, 1965; EA DiMarzio, FL McCrackin. J Chem Phys 43:539, 1965; C Hoeve, EA DiMarzio, P Peyser. J Chem Phys 42:2558, 1965.
17. RJ Rubin. J Chem Phys 43:2392, 1965.
18. IS Jones, P Richmond. J Chem Soc, Faraday Trans 2:73, 1977.
19. JN Israelachvili. Intermolecular and Surface Forces. London: Academic Press, 1992.
20. M Daoud, PG de Gennes. J Phys (France) 38:85, 1977.
21. PG de Gennes. Rep Prog Phys 32:187, 1969.
22. PJ Flory. Statistical Mechanics of Chain Molecules. Munich: Hanser Press, 1988.
23. JMJ van Leeuwen, HJ Hilhorst. Physica A 107:319, 1981; TW Burkhardt. J Phys A 14:L63, 1981; DM Kroll. Z Phys B 41:345, 1981.
24. R Lipowsky, A Baumgärtner. Phys Rev A 40:2078, 1989; R Lipowsky. Physica Scripta T29:259, 1989.
25. RR Netz. Phys Rev E 51:2286, 1995.
26. OV Borisov, EB Zhulina, TM Birshtein. J Phys II (France) 4:913, 1994.
27. X Châtellier, TJ Senden, JF Joanny, JM di Meglio. Europhys Lett 41:303, 1998.
28. JF Joanny. J Phys II France 4:1281, 1994; AV Dobrynin, M Rubinstein, JF Joanny. Macromolecules 30:4332, 1997.
29. RR Netz, JF Joanny. Macromolecules 31:5123, 1998.
30. PG de Gennes. Phys Lett A 38:339, 1972.
31. E Eisenriegler, K Kremer, K Kinder. J Chem Phys 77:6296–6320, 1982; E Eisenriegler. J Chem Phys 79:1052–1064, 1983.
32. PG de Gennes. J Phys (Paris) 37:1445–1452, 1976.
33. PG de Gennes, P Pincus. J Phys Lett (Paris) 44:L241–L246, 1983.
34. E Bouchaud, M Daoud. J Phys (Paris) 48:1991–2000, 1987.
35. JW Cahn, JE Hilliard. J Chem Phys 28:258–267, 1958.
36. PG de Gennes. Macromolecules 14:1637–1644, 1981.
37. O Guiselin. Europhys Lett 17:225–230, 1992.
38. L Auvray, JP Cotton. Macromolecules 20:202, 1987.
39. LT Lee, O Guiselin, B Farnoux, A Lapp. Macromolecules 24:2518, 1991; O Guiselin, LT Lee, B Farnoux, A Lapp. J Chem Phys 95:4632, 1991; O Guiselin. Europhys Lett 1:57, 1992.
40. JMHM Scheutjens, GJ Fleer, MA Cohen Stuart. Colloids Surfaces 21:285, 1986; GJ Fleer, JMHM Scheutjens, MA Cohen Stuart. Colloids Surfaces 31:1, 1988.
41. A Johner, JF Joanny, M Rubinstein. Europhys Lett 22:591, 1993.
42. AN Semenov, JF Joanny. Europhys Lett 29:279, 1995; AN Semenov, J Bonet-Avalos, A Johner, JF Joanny. Macromolecules 29:2179, 1996; A Johner, J Bonet-Avalos, CC van der Linden, AN Semenov, JF Joanny. Macromolecules 29:3629, 1996.
43. AN Semenov, JF Joanny, A Johner. In: A Grosberg, ed. Theoretical and Mathematical Models in Polymer Research. Boston: Academic Press, 1998.
44. JF Joanny, L Leibler, PG de Gennes. J Polym Sci: Polym Phys Ed 17:1073–1084, 1979.

45. PG de Gennes. Macromolcules 15:492–500, 1982.
46. JMHM Scheutjens, GJ Fleer. Macromolecules 18:1882, 1985; GJ Fleer, JMHM Scheutjens. J Coll Interface Sci 111:504, 1986.
47. J Bonet Avalos, JF Joanny, A Johner, AN Semenov. Europhys Lett 35:97, 1996; J Bonet Avalos, A Johner, JF Joanny. J Chem Phys 101:9181, 1994.
48. J Klein, PF Luckham. Nature 300:429, 1982; Macromolecules 17:1041–1048, 1984.
49. J Klein, PF Luckham. Nature 308:836, 1984; Y Almog, J Klein. J Colloid Interface Sci 106:33, 1985.
50. G Rossi, PA Pincus. Europhys Lett 5:641, 1988; Macromolecules 22:276–283, 1989.
51. J Klein. Nature 288:248, 1980; J Klein, PF Luckham. Macromolecules 19:2007–2010, 1986.
52. J Klein, P Pincus. Macromolecules 15:1129, 1982; K Ingersent, J Klein, P Pincus. Macromolecules 19:1374–1381, 1986.
53. K Ingersent, J Klein, P Pincus. Macromolecules 23:548–560, 1990.
54. PF Luckham, J Klein. Macromolecules 18:721–728, 1985.
55. J Klein, G Rossi. Macromolecules 31:1979–1988, 1998.
56. I Borukhov, D Andelman, H Orland. Eur Phys J B 5:869–880, 1998.
57. MA Cohen Stuart. J Phys (France) 49:1001–1008, 1988.
58. MA Cohen Stuart, GJ Fleer, J Lyklema, W Norde, JMHM Scheutjens. Adv Colloid Interface Sci 34:477–535, 1991.
59. JL Barrat, JF Joanny. Europhys Lett 24:333, 1993.
60. RR Netz, H Orland. Eur Phys J B 8:81, 1999.
61. RR Netz, JF Joanny. Macromolecules 32:9013, 1999.
62. I Borukhov, D Andelman, H Orland. Europhys Lett 32:499, 1995; Macromolecules 31:1665–1671, 1998; J Phys Chem B 103:5042–5057, 1999.
63. G Decher. Science 277:1232, 1997; M Lösche, J Schmitt, G Decher, WG Bouwman, K Kjaer. Macromolecules 31:8893, 1998.
64. E Donath, GB Sukhorukov, F Caruso, SA Davis, H Möhwald. Angew Chem Int Ed 16:37, 1998; GB Sukhorukov, E Donath, SA Davis, H Lichtenfeld, F Caruso, VI Popov, H Möhwald. Polym Adv Technol 9:759, 1998.
65. F Caruso, RA Caruso, H Möhwald. Science 282:1111, 1998; F Caruso, K Niikura, DN Furlong, Y Okahata. Langmuir 13:3422, 1997.
66. JF Joanny. Eur Phys J B 9:117, 1999.
67. HA van der Schee, J Lyklema. J Phys Chem 88:6661, 1984; J Papenhuijzen, HA van der Schee, GJ Fleer. J Colloid Interface Sci 104:540, 1985; OA Evers, GJ Fleer, JHMH Scheutjens, J Lyklema. J Colloid Interface Sci 111:446, 1985; HGM van de Steeg, MA Cohen Stuart, A de Keizer, BH Bijsterbosch. Langmuir 8:8, 1992.
68. P Linse. Macromolecules 29:326, 1996.
69. M Muthukumar. J Chem Phys 86:7230, 1987.
70. R Varoqui, A Johner, A Elaissari. J Chem Phys 94:6873, 1991; R Varoqui. J Phys II (France) 3:1097, 1993.
71. PG de Gennes. J Phys Chem 94:8407, 1990.
72. D Andelman, JF Joanny. Macromolecules 24:6040–6041, 1991; JF Joanny, D Andelman. Makromol Chem Macromol Symp 62:35–41, 1992; D Andelman, JF Joanny. J Phys II (France) 3:121–138, 1993.
73. V Aharonson, D Andelman, A Zilman, PA Pincus, E Raphaël. Physica A 204:1–16, 1994; 227:158–160, 1996.
74. RR Netz, D Andelman, H Orland. J Phys II (France) 6:1023–1047, 1996.
75. X Châtellier, D Andelman. Europhys Lett 32:567–572, 1995; X Châtellier, D Andelman. J Phys Chem 22:9444–9455, 1996.
76. TA Vilgis, G Heinrich. Macromolcules 27:7846, 1994; G Huber, TA Vilgis. Eur Phys J B 3:217, 1998.

77. D Hone, H Ji, PA Pincus. Macromolecules 20:2543, 1987; H Ji, D Hone. Macromolecules 21:2600, 1988.
78. M Blunt, W Barford, R Ball. Macromolcules 22:1458, 1989.
79. CM Marques, JF Joanny. J Phys (France) 49:1103, 1988.
80. JT Brooks, CM Marques, ME Cates. Europhys Lett 14:713, 1991; J Phys II (France) 1:673, 1991; F Clement, JF Joanny. J Phys II (France) 7:973, 1997.
81. F von Goeler, M Muthukumar. J Chem Phys 100:7796, 1994.
82. T Wallin, P Linse. Langmuir 12:305, 1996; J Phys Chem 100:17873, 1996; J Phys Chem B 101:5506, 1997.
83. E Gurovitch, P Sens. Phys Rev Lett 82:339, 1999.
84. EM Mateescu, C Jeppesen, P Pincus. Europhys Lett 46:493, 1999.
85. RR Netz, JF Joanny. Macromolecules 32:9026, 1999.
86. A Halperin, JF Joanny. J Phys II (France) 1:623, 1991.
87. CM Marques, JF Joanny. Macromolecules 23:268, 1990; B van Lent, JMHM Scheutjens. J Phys Chem 94:5033, 1990; JP Donley, GH Fredrickson. Macromolecules 27:458, 1994.
88. P Auroy, L Auvray, L Leger. Phys Rev Lett 66:719, 1991; Macromolecules 24:2523, 1991; Macromolecules 24:5158, 1991.
89. HJ Taunton, C Toprakcioglu, LJ Fetters, J Klein. Nature 332:712, 1988; Macromolecules 23:571, 1990.
90. JB Field, C Toprakcioglu, L Dai, G Hadziioannou, G Smith, W Hamilton. J Phys II (France) 2:2221, 1992.
91. CM Marques, JF Joanny, L Leibler. Macromolecules 21:1051, 1988. CM Marques, JF Joanny. Macromolecules 22:1454, 1989.
92. MS Kent, LT Lee, B Farnoux, F Rondelez. Macromolecules 25:6240, 1992; MS Kent, LT Lee, BJ Factor, F Rondelez, GS Smith. J Chem Phys 103:2320, 1995; HD Bijsterbosch, VO de Haan, AW de Graaf, M Mellema, FAM Leermakers, MA Cohen Stuart, AA van Well. Langmuir 11: 4467, 1995; MC Fauré, P Bassereau, MA Carignano, I Szleifer, Y Gallot, D Andelman. Eur Phys J B 3:365, 1998.
93. R Teppner, M Harke, H Motschmann. Rev Sci Instrum 68:4177, 1997; R Teppner, H Motschmann. Macromolecules 31:7467, 1998.
94. PG de Gennes. Macromolecules 13:1069, 1980.
95. S Alexander. J Phys (France) 38:983, 1977.
96. A Halperin, M Tirell, TP Lodge. Adv Polym Sci 100:31, 1992.
97. T Cosgrove, T Heath, B van Lent, F Leermakers, J Scheutjens. Macromolecules 20:1692, 1987.
98. M Murat, GS Grest. Macromolecules 22:4054, 1989; A Chakrabarti, R Toral. Macromolecules 23:2016, 1990; PY Lai, K Binder. J Chem Phys 95:9288, 1991.
99. AN Semenov. Sov Phys JETP 61:733, 1985.
100. ST Milner, TA Witten, ME Cates. Europhys Lett 5:413, 1988; Macromolecules 21:21610, 1988; ST Milner. Science 251:905, 1991.
101. AM Skvortsov, IV Pavlushkov, AA Gorbunov, YB Zhulina, OV Borisov, VA Pryamitsyn. Polym Sci 30:1706, 1988.
102. RR Netz, M Schick. Europhys Lett 38:37, 1997; Macromolecules 31:5105, 1998.
103. C Seidel, RR Netz. Macromolecules 33:634, 2000.
104. MA Carignano, I Szleifer. J Chem Phys 98:5006, 1993; J Chem Phys 100:3210, 1994; Macromolecules 28:3197, 1995; J Chem Phys 102:8662, 1995. A detailed summary of tethered layers is given in I Szleifer, MA Carignano. Adv Chem Phys XCIV:165, 1996.
105. GS Grest. Macromolecules 27:418, 1994.
106. TA Witten, PA Pincus. Macromolecules 19:2509, 1986; EB Zhulina, OV Borisov, VA Priamitsyn. J Colloid Surface Sci 137:495, 1990.
107. ST Milner. Europhys Lett 7:695, 1988.

108. ST Milner, TA Witten, ME Cates. Macromolecules 22:853, 1989.
109. A Halperin. J Phys (France) 49:547, 1988; YB Zhulina, VA Pryamitsyn, OV Borisov. Polym Sci 31:205, 1989; EB Zhulina, OV Borisov, VA Pryamitsyn, TM Birshtein. Macromolecules 24:140, 1991; DRM Williams. J Phys II (France) 3:1313, 1993.
110. P Auroy, L Auvray. Macromolecules 25:4134, 1992.
111. JF Marko. Macromolecules 26:313, 1993.
112. PY Lai, K Binder. J Chem Phys 97:586, 1992; GS Grest, M Murat. Macromolecules 26:3108, 1993.
113. M Daoud, JP Cotton. J Phys (France) 43:531, 1982.
114. RC Ball, JF Marko, ST Milner, AT Witten. Macromolecules 24:693, 1991; H Li, TA Witten. Macromolecules 27:449, 1994.
115. N Dan, M Tirrell. Macromolecules 25:2890, 1992.
116. M Murat, GS Grest. Macromolecules 24:704, 1991.
117. ST Milner, TA Witten. J Phys (France) 49:1951, 1988.
118. TM Allen, C Hansen, F Martin, C Redemann, A Yau-Young. Biochim Biophys Acta 1006:29, 1991; MJ Parr, SM Ansell, LS Choi, PR Cullis. Biochim Biophys Acta 1195:21, 1994.
119. R Lipowsky. Europhys Lett 30:197, 1995; C Hiergeist, R Lipowsky. J Phys II (France) 6:1465, 1996; C Hiergeist, VA Indrani, R Lipowsky. Europhys Lett 36:491, 1996; M Breidenich, RR Netz, R Lipowsky. Europhys Lett 49:431, 2000.
120. M Aubouy, GH Fredrickson, P Pincus, E Raphael. Macromolecules 28:2979, 1995.
121. AP Gast, L Leibler. Macromolecules 19:686, 1986.
122. P Pincus. Macromolecules 24:2912, 1991; OV Porisov, TM Birshtein, EB Zhulina. J Phys II (France) 1:521, 1991; F Csaijka, RR Netz, C Seidel. Eur Phys J E 4:505, 2001.
123. JF Marko, TA Witten. Phys Rev Lett 66:1541, 1991.
124. G Brown, A Chakrabarti, JF Marko. Macromolecules 28:7817, 1995; EB Zhulina, C Singhm, AC Balazs. Macromolecules 29:8254, 1996.
125. A Halperin, S Alexander. Europhys Lett 6:329, 1988; A Johner, JF Joanny. Macromolecules 23:5299, 1990; C Ligoure, L Leibler. J Phys (France) 51:1313, 1990; ST Milner. Macromolecules 25:5487, 1992; A Johner, JF Joanny. J Chem Phys 98:1647, 1993.